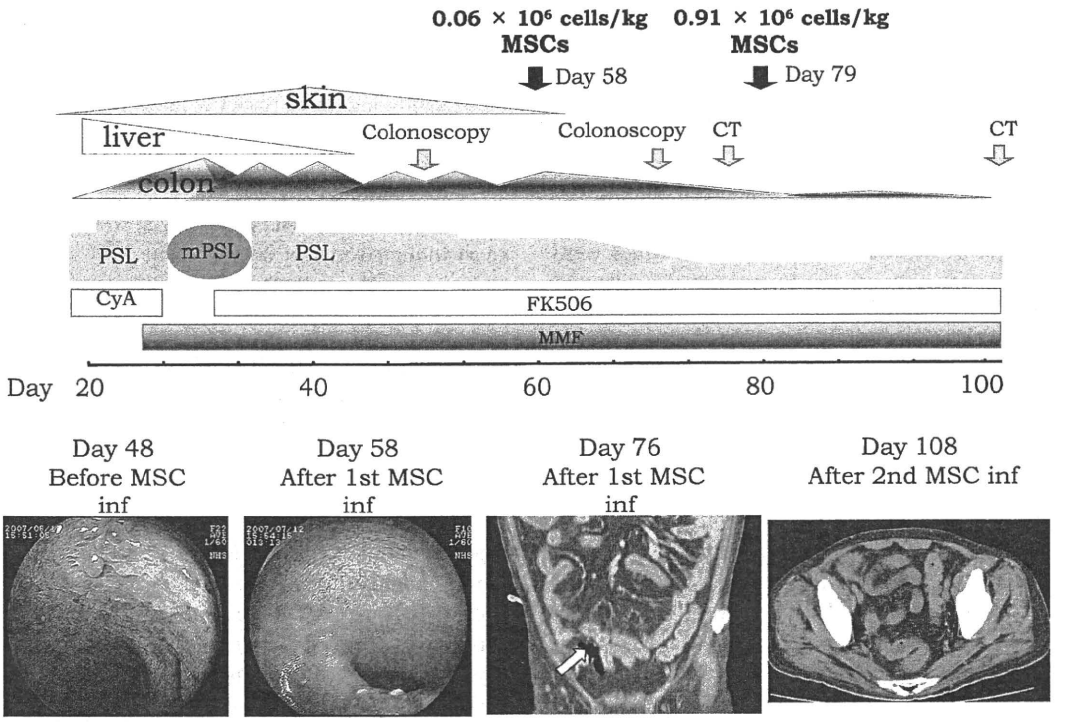

Fig. 2. Clinical course of the patient. MSCs, mesenchymal stromal cells ; MSC inf, MSC infusion ; CyA, cyclosporine ; FK506, tacrolimus ; MMF, mycophenolate mofetil ; PSL, prednisolne ; mPSL, methylprednisolone ; CT, computed tomography. *The white arrow* indicates free-air due to the intestinal perforation.

the area surrounding the small intestine due to perforation of the intestine. To resolve the gut aGVHD and repair the intestinal mucosa, 0.91 × 10^6/kg of fresh MSCs were infused on day 79. After the second administration of MSCs, the abdominal free-air disappeared and bloody stools decreased. The patient was able to ingest orally. Since the abdominal pain and bloody diarrhea did not completely disappear, infliximab was given on day 153. Although the patient was discharged on day 178, he died of septic shock on day 193.

There are two reports on using MSCs as a first line treatment for aGVHD (Table 2). Kebriaei *et al.* reported treatment of aGVHD with a combination of steroids and third-party MSCs (Procymal).[42] Patients were randomized to either a high-dose MSC group (8 × 10^6/kg) or a low dose MSC group (2 × 10^6/kg). The number of patients and the median age in the former group were 15 and 49 years, respectively, while those in the latter group were 16 and 53 years, respectively. There was no difference between the two groups in the overall CR rate and in the CR rate according to the organ system of aGVHD. Osiris conducted a phase III trial of MSCs (Procymal) plus steroid as a first line treatment for aGVHD (protocol 265). One hundred and ninety-two patients were enrolled but the results have not been released.[43]

None of the above reports mentioned above showed immediate or late adverse effects associated with MSC infusions such as infusion reactions, pulmonary embolisms, transmissions of infectious agents, and ectopic mass formation derived from the infused MSCs. Since MSCs are suggested not to cause systemic immunosuppression, it is likely that the graft-versus-leukemia (GVL) reaction is not impaired and the frequency and severity of systemic infections do not increase after MSC therapy. Indeed, none of the above reports indicated a significant increase in relapse or infections after MSC therapy. The effects of MSCs on aGVHD seem not to be associated with MSC origins, i.e., HLA-identical siblings, haploidentical family donors, HLA-matched unrelated donors, and HLA-mismatched (third party) donors. Because it takes time to obtain MSCs by culture, frozen MSCs from third party donors are most suitable for the treatment of aGVHD. MSCs seem to be useful for steroid-resistant aGVHD as a second line therapy, especially for children and for gut aGVHD. In Japan, a phase I/II study of MSCs from third party donors to treat steroid-resistant aGVHD is being conducting.

MSCs for prevention of graft failure, enhancement of engraftment, and prevention of GVHD

MSCs were cotransplanted with HSCs to prevent graft failure, enhance engraftment, and reduce GVHD (Table 3). A first case was reported by Lee *et al.* in 2002.[44] A 20-year-old woman with high-risk AML was transplanted with peripheral blood $CD34^+$ cells from her haploidentical father with bone marrow-derived MSCs from the same donor. Engraftment was rapid and no GVHD occurred. Lazarus *et al.* reported the cotransplantation of HSCs from HLA-identical siblings with bone marrow-derived MSCs from HLA-identical siblings.[45] Nineteen patients and 27 patients received bone marrow transplants and peripheral blood stem cell transplants, respectively. The GVHD prophylaxis was short-term methotrexate and cyclosporine treatment. The infused MSC dose was 1.0×10^6/kg for 18 patients, 2.5×10^6/kg for 19 patients, and 5.0×10^6/kg for 5 patients. Neutrophil engraftment and platelet engraftment took 14.0 days and 20.5 days, respectively. aGVHD was observed in 23 patients (50%), of whom 13 (28%) showed grade II to IV aGVHD. Of 21 evaluable patients, 14 and 8 patients had limited and extensive cGVHD, respectively. Relapse or disease progression occurred in 12 patients. Differences between the doses of MSCs in clinical outcomes were not apparent. This study did not show significant rapid engraftment of HSCs or reduction of GVHD. Le Blanc *et al.* reported seven patients with cotransplantation of HSCs with bone marrow-derived MSCs.[46] MSC donors were HLA-identical siblings or haploidentical relatives. The infused MSC dose was 1×10^6/kg. Three patients had received HSC transplants before the cotransplantation of HSCs and MSCs. Engraftment of the three patients was shown. The cotransplantation of haploidentical HSCs with MSCs was reported by Ball *et al.*[47] The patients were children with the median age of 8 years. They received peripheral blood $CD34^+$ cells from haploidentical relatives, followed by bone marrow-derived MSCs from the same donors. The mean dose of MSCs was 1.6×10^6/kg. Engraftment was rapid and graft failure did not occur. aGVHD was shown in 2 patients (14%) for grade I to II, while cGVHD was shown in one patient (7%). These results were not significantly better than historical controls. Ning *et al.* conducted a randomized study comparing HSCT with HSCT plus MSC transplantation.[48] Both HSCT donors and MSC transplantation donors were HLA-identical siblings. The HSCT sources were bone marrow in 9 patients, peripheral blood stem cells in 13 patients, and bone marrow combined with peripheral blood stem cells in 3 patients. Fifteen patients underwent HSCT only, while 10 patients underwent the cotransplantation of HSCs with MSCs. The median infused MSC dose was 0.33×10^6/kg. Neutrophil engraftment in the HSCT group and the cotransplantation group took 15 and 16 days, respectively. Platelet engraftment in the former and the latter took 27 and 30 days, respectively. Only grade I or II aGVHD occurred in 11 patients of the former group and 4 patients of the latter group, respectively. cGVHD was shown in 4 of 14 patients in the former and one of 7 patients in the latter, respectively. Infection frequencies did not differ between the two groups. Notably, 3 patients in the former group relapsed (20%), while 6 patients in the latter relapsed (60%). Relapse was not associated with the infused MSC dose. Zang *et al.* examined hematological recovery and GVHD severity in patients receiving HSC transplants plus MSC infusions.[49] Twelve patients received peripheral blood stem cell transplants from HLA-identical siblings, followed by MSC infusions from the same donors. The infused doses of peripheral blood $CD34^+$ cells and MSCs were 4.34×10^6/kg and 1.48×10^6/kg, respectively. The GVHD prophylaxis was short-term methotrexate and cyclosporine treatment. Engraftment was rapid; neutrophil and platelet engraftments took 11 and 13.5 days, respectively. Seven and 2 patients developed grade I and grade III/IV aGVHD, respectively. cGVHD was shown in 4 patients. Relapse occurred in 4 patients (30%) including one with chronic myelogeneous leukemia (CML) in an accelerated phase, one with CML in blastic transformation, one with AML in second remission and one with ALL in second remission. Seven patients were alive and 5 patients were dead because of relapse or infection. Gonzzalo-Paganzo *et al.* reported an unique clinical trial of the combined transplantation of cord blood, peripheral blood stem cells from unrelated donors, and bone marrow-derived MSCs from the same peripheral blood stem cell donors.[50] Engraftment and aGVHD severity of the patients were similar to those in control patients.

No adverse effect associated with MSCs was not reported in the above studies. Cotransplantation of HSCs with MSCs seems not to markedly enhance neutrophil and platelet engraftments, as compared with historical controls. However, in cases with a risk of graft failure such as heavily transfused patients with aplastic anemia and patients with a history of graft failure, cotransplantation of HSCs with MSCs may accelerate engraftment of the HSCs. Unfortunately, cotransplantation of HSCs with MSCs does not seem to reduce aGVHD. This may be because MSCs do not effect unstimulated lymphocytes before the onset of aGVHD. Further studies are needed of the efficacy of cotransplanted MSCs for the acceleration of HSC engraftment and aGVHD prevention.

MSCs for cGVHD and tissue repair

A few patients with cGVHD treated with MSCs were reported with variable responses.[35,38] Very recently, Zhou *et al.* reported the efficacy of bone marrow-derived MSCs for 4 patients with sclerodermatous cGVHD.[51] MSCs were administered by intrabone marrow injection. Following an increase in Th1 lymphocytes and decrease in Th2 lymphocytes, symp-

Table 3. Cotransplantation of hemopoietic stem cells with mesenchymal stroma cells to prevent graft failure and/or graft-versus-host disease

1 st author	Year of publication	Ref	No. of Pts	Age (Years)	No. of BM-MNCs ($\times 10^8$/kg)	No. of PB-CD 34$^+$ ($\times 10^6$/kg)	No. of MSC dose ($\times 10^6$/kg)	Neut engraft (Days)	Plt engraft (Days)	No. of graft failure	No. of pts with of aGVHD I/II/III/IV (%)	No. of pts with cGVHD Limited/Extensive	No. of relapse (%)
Lee	2002	44	1	20	ND	5.7	1.5	12	15	none	none	none	none
Lazarus	2005	45	46	44.5	3.6	5	1.0 (18 pts), 2.5 (19 pts), 5 (5 pts)	14	20.5	0	3 (7)/13 (28)/5 (11)/2 (4)	14/8	12 (26)[¶]
Le Blanc	2007	46	7	12	NS	7.2[§]	1	12	12[†]	0	4 (57)/2 (29)/0/0	1/0	0
Ball	2007	47	14	8	ND	21.5	1.6	12	10	0	2 (I+II, 14)/0 (III+IV, 0)	1/0	2
Ball[#]	2007	47	47	7.1	ND	24.3	ND	13	13	7	12 (I+II, 26)/2 (III+IV, 4)	4/2	ND
Ning	2008	48	10	38	5.3 (4 pts)	5.4 (6 pts)	0.33	16	30	0	3 (30)/1 (10)/0/0	1/0	6 (60)
Ning[#]	2008	48	15	37	4.4 (5 pts)	5.1 (10 pts)	ND	15	27	0	3 (20)/8 (53)/0/0	1/1	3 (20)
Zhang	2009	49	12	38.5	ND	4.34	1.48	11	13.5	0	7 (58)/1 (II-III, 8)/1 (8)/0	2/2	4 (30)
Gonzalo-Daganzo	2009	50	9	32	ND	0.12[§]	1.2	12	44	0	1 (11)/4 (44)/0/0	1/0	1 (11)
Gonzalo-Daganzo[#]	2009	50	46	35	ND	0.10[§]	ND	10	32	ND	18 (37)/5 (11)/3 (7)/3 (7)	8/3	6 (13)

Ref, references ; Pts, patients ; No., number ; BM-MNCs, bone marrow nucleated cells ; PB-CD 34$^-$, peripheral blood CD 34$^+$ cells ; MSC, mesenchymal stromal cells ; Neut Engraft, days of neutrophil count greater than 0.5×10^9/L ; Plt engraft, days of platelet count greater than 20×10^9/L ; aGVHD, acute graft-versus-host-disease ; cGVHD, chronic graft-versus-host disease ; [¶], including progression ; ND, not done or not shown ; [§], including the cases of bone marrow and cord blood cells ; [†], days of platelet count greater than 30×10^9/L ; [§], cord blood ; [#], controls

toms of the patients improved. No adverse effects associated with MSC infusions were noted. It is necessary to clarify whether MSCs are effective against cGVHD and which route of injection is better, a conventional intravenous injection or an intrabone marrow injection.

MSCs are shown to have the ability to repair damaged tissue by homing to damaged sites and differentiating into the cells of that tissue.[10,35] A clinical trial was conducted to repair damaged tissue associated with HSCT or aGVHD using MSCs.[52] Infusions led to a dramatic resolution of hemorrhagic cystitis, gut perforation and pneumothorax after HSCT. Our case, as shown in Fig. 2, showed a resolution of intestinal perforation associated with gut aGVHD on the infusion of MSCs. Although it is not clear which damaged tissues or organs MSCs can repair, MSCs have a promising future to treat damaged tissue following HSCT.

CONCLUSIONS AND FUTURE DIRECTIONS

MSCs lead to a normalization of the immune system in stimulated mice and humans via inhibition of T cell proliferation, inhibition of inflammatory cytokine production, increase of Treg cells and correction of the Th1/Th2 balance. However, the mechanisms of MSC-mediated T cell suppression are complex and remain unclear. Efforts to clarify the factors or molecules associated with MSC-mediated T cell suppression should be continued, since direct medication to suppress T cell proliferation could be used instead of MSCs. MSCs seem not to suppress the whole immune system but specifically aGVHD without impairment of the GVL effect in leukemia patients. However, there are many unsolved problems in the treatment of GVHD with bone marrow-derived MSCs; the source of MSCs, i.e., the same HSCT donors, haploidentical donors or third party donors, the single dose of MSCs, the total dose of MSCs and the interval of MSC administration. It is unclear whether MSCs preferentially suppress gut aGVHD or aGVHD in pediatric patients. Although there have been no reports on direct MSC-related adverse effects such as infusion reactions, pulmonary embolisms, pathogen transmissions and ectopic tumor formation, careful observations and long-term follow-up for patients receiving MSCs are needed. Finally, both basic researching MSCs and clinical trials using MSCs will lead to bring a better understanding of MSCs in the field of clinical immunology and hematology.

ACKNOWLEDGMENTS

The authors thank doctors and medical technologists for the clinical trials using MSCs in our hospital.

REFERENCES

1 Pittenger MF, Mackay AM, Beck SC, Jaiswal RK, Douglas R, *et al.*: Multilineage potential of adult human mesenchymal stem cells. Science 284: 143-147, 1999
2 Gronthos S, Franklin DM, Leddy HA, Robey PG, Storms RW, *et al.*: Surface protein characterization of human adipose tissue-derived stromal cells. J Cell Physiol 189: 54-63, 2001
3 Campagnoli C, Roberts IA, Kumar S, Bennett PR, Bellantuono I, *et al.*: Identification of mesenchymal stem/progenitor cells in human first-trimester fetal blood, liver, and bone marrow. Blood 98: 2396-2402, 2001
4 Igura K, Zhang X, Takahashi K, Mitsuru A, Yamaguchi S, *et al.*: Isolation and characterization of mesenchymal progenitor cells from chorionic villi of human placenta. Cytotherapy 6: 543-553, 2004
5 Tocci A, Forte L: Mesenchymal stem cells: use and perspectives. Hematol J 4: 92-96, 2003
6 Horwitz EM, Gordon PL, Koo WK, Marx JC, Neel MD, *et al.*: Isolated allogeneic bone marrow-derived mesenchymal cells engraft and stimulate growth in children with osteogenesis imperfecta: implications for cell therapy of bone. Proc Natl Acad Sci U S A 99: 8932-8937, 2002
7 Koc IN, Gerson SL, Cooper BW, Dyhouse SM, Haynesworth SE, *et al.*: Rapid hematopoietic recovery after coinfusion of autologous-blood stem cells and culture-expanded marrow mesenchymal stem cells in advanced breast cancer patients receiving high-dose chemotherapy. J Clin Oncol 18: 307-316, 2000
8 Noort WA, Kruisselbrink AB, in't Anker PS, Kruger M, van Bezooijen RL, *et al.*: Mesenchymal stem cells promote engraftment of human umbilical cord blood-derived CD34$^+$ cells in NOD/SCID mice. Exp Hematol 30: 870-878, 2002
9 in't Anker PS, Noort WA, Kruisselbrink AB, Scherjon SA, Beekhuizen W, *et al.*: Nonexpanded primary lung bone marrow-derived mesenchymal cells promote the engraftment of umbilical cord blood-derived CD34$^+$ cells in NOD/SCID mice. Exp Hematol 31: 881-889, 2003
10 Le Blanc K, Rasmusson I, Sundberg B, Götherström C, Hassan M, *et al.*: Treatment of severe acute graft-versus-host disease with third party haploidentical mesenchymal stem cells. Lancet 363: 1439-1441, 2004
11 Le Blanc K, Frassoni F, Ball L, Locatelli F, Roelofs H, *et al.*: Mesenchymal stem cells for treatment of steroid-resistant, severe, acute graft-versus-host disease: a phase II study. Lancet 371: 1579-1586, 2008
12 Ren G, Su J, Zhang L, Zhao X, Ling W, *et al.*: Species variation in the mechanisms of mesenchymal stem cell-mediated immunesuppression. Stem Cells 27: 1954-1962, 2009
13 Peister A, Mellad JA, Larson BL, Hall BM, Gibson LF, *et al.*: Adult stem cells from bone marrow (MSCs) isolated from different stains of inbred mice vary in surface epitopes, rates of proliferation, and differentiation potential. Blood 103: 1662-1668, 2004
14 Colter DC, Class R, DiGirolamo CM, Prockop DJ: Rapid expan-

sion of recycling stem cells in cultures of plastic-adherent cells from human bone marrow. Proc Natl Acad Sci U S A 28 : 3213-3218, 2000
15 Di Nicola M, Cario-Stella C, Magni M, Milanesi M, Longoni PD, *et al.* : Human bone marrow stromal cells suppress T-lymphocyte proliferation induced by cellular or nonspecific mitogenic stimuli. Blood 99 : 3838-3843, 2002
16 Krampera M, Glennie S, Dyson J, Scott D, Laylor R, *et al.* : Bone marrow mesenchymal stem cells can inhibit the response of naïve and memory antigen-specific T cells to their cognate peptide. Blood 101 : 3722-3729, 2003
17 Meisel R, Zibert A, Laryea M, Göbel U, Däubener W, *et al.* : Human bone marrow stromal cells inhibit allogenic T-cell responses by indoleamine 2, 3-dioxygenase-mediated tryptophan degradation. Blood 103 : 4619-4621, 2004
18 Glennie S, Soeiro I, Dyson PJ, Lam EW, Dazzi F : Bone marrow mesenchymal stem cells induce division arrest anergy of activated T-cells. Blood 105 : 2821-2827, 2005
19 Aggarwal S, Pittenger MF : Human mesenchymal stem cells modulate allogeneic immune cells responses. Blood 105 : 1815-1822, 2005
20 Sato K, Ozaki K, Oh I, Meguro A, Hatanaka K, *et al.* : Nitric oxide plays a critical role in suppression of T-cell proliferation by mesenchymal stem cells. Blood 109 : 228-234, 2007
21 Corcione A, Benvenuto F, Ferretti E, Giunti D, Cappiello V, *et al.* : Human mesenchymal stem cells modulate B-cell functions. Blood 107 : 367-372, 2006
22 Spaggiari GM, Capobianco A, Becchetti S, Mingari MC, Moretta L : Mesenchymal stem cell-natural killer cell interactions : evidence that activated NK cells are capable of killing MSCs, whereas MSCs can inhibit IL-2 induced NK-cell proliferation. Blood 107 : 1484-1490, 2006
23 Jiang XX, Zhang Y, Liu B, Zhang SX, Wu Y, *et al.* : Human mesenchymal stem cells inhibit differentiation and function of monocyte-derived dendritic cells. Blood 105 : 4120-4126, 2005
24 Suniara RK, Jenkinson EJ, Owen JJ : An essential role for thymic mesenchyme in early T cell development. J Exp Med 191 : 1051-1056, 2000
25 Djouad F, Plence P, Bony C, Tropel P, Apparailly F, *et al.* : Immunosuppressive effect of mesenchymal stem cells favors tumor growth in allogenic animals. Blood 102 : 3837-3844, 2003
26 Le Blanc K, Rasmusson I, Gotherstrom C, Seidel C, Sundberg B, *et al.* : Mesenchymal stem cells inhibit the expression of CD25 (interleukin-2 receptor) and CD38 on pythohaemagglutinin-activated lymphocytes. Scand J Immunol 60 : 307-315, 2004
27 Groh ME, Maitra B, Szekely E, Koç ON : Human mesenchymal stem cells require monocyte-mediated activation to suppress alloreactive T cells. Exp Hematol 33 : 928-934, 2005
28 Fowler DH, Kurasawa K, Smith R, Eckhaus MA, Gress RE : Donor CD4-enriched cells of Th2 cytokine phenotype regulate graft-versus-host disease without impairing allogenic engraftment in sublethally irradiated mice. Blood 84 : 3540-3549, 1994
29 Pan L, Delmonte J Jr, Jalonen CK, Ferrara JL : Pretreatment of donor mice with granulocyte colony-stimulating factor polarizes donor T lymphocytes toward type-2 cytokine production and reduces severity of experimental graft-versus-host disease. Blood 86 : 4422-4429, 1995
30 Oh I, Ozaki K, Sato K, Meguro A, Tatara R, *et al.* : Interferon-γ and NF-κB mediate nitric oxide production by mesenchymal stromal cells. Biochem Biophys Res Commun 355 : 956-962, 2007
31 Nguyen VH, Shashidhar S, Chang DS, Ho L, Kambham N, *et al.* : The impact of regulatory T cells on T-cell immunity following hematopoietic cell transplantation. Blood 111 : 945-953, 2008
32 Yi T, Zhao D, Lin CL, Zhang C, Chen Y, *et al.* : Absence of donor Th17 leads to augmented Th1 differentiation and exacerbated acute graft-versus-host disease. Blood 112 : 2101-2110, 2008
33 Carlson MJ, West ML, Coghill JM, Panoskaltsis-Mortari A, Blazar BR, *et al.* : *In vitro*-differentiated TH17 cells mediate lethal acute graft-versus-host disease with severe cutaneous and pulmonary manifestations. Blood 113 : 1365-1374, 2009
34 Tatara R, Ozaki K, Oh I, Hatanaka K, Meguro A, Matsu H, *et al.* : Mesenchymal stem cells inhibit Th17 differentiation through PGE2 production. Blood 114 : 1403, 2009 (*Abstract*)
35 Ringdén O, Uzunel M, Rasmusson I, Remberger M, Sundberg B, *et al.* : Mesenchymal stem cells for treatment of therapy-resistant graft-versus-host disease. Transplantation 81 : 1390-1397, 2006
36 Prasad VK, Lucas KG, Kleiner GI, Talano JAM, Jacobsohn D, *et al.* : Use of mesenchymal stem cells to treat pediatric patients with severe (Grade III-IV) acute graft versus host disease refractory to steroid and other agents on a compassionate use basis. Blood 110 : 2971, 2007 (*ASH Annual Meeting Abstracts*)
37 Fang B, Song Y, Liao L, Zhang Y, Zhao RC : Favorable response to human adipose tissue-derived mesenchymal stem cells in steroid-refractory acute graft-versus-host disease. Transplant Proc 39 : 3358-3362, 2007
38 Müller I, Kordowich S, Holzwarth C, Isensee G, Lang P, *et al.* : Application of multipotent mesenchymal stromal cells in pediatric patients following allogeneic stem cell transplantation. Blood Cells Mol Dis 40 : 25-32, 2008
39 von Bonin M, Stölzel F, Goedecke A, Richter K, Wuschek N, *et al.* : Treatment of refractory acute GVHD with third-party MSC expanded in platelet lysate-containing medium. Bone Marrow Transplant 43 : 245-251, 2009
40 Osiris Therapeutics Announces Preliminary Results for Prochymal Phase III GvHD Trials. http://investor.osiris.com/releasedetail.cfm?ReleaseID=407404
41 Muroi K : Treatment of GVHD with mesenchymal stromal cells. Japanese Journal of Transfusion and Cell Therapy 55 : 182, 2009 (*in Japanese, Abstract*)
42 Kebriaei P, Isola L, Bahceci E, Holland K, Rowley S, *et al.* : Adult human mesenchymal stem cells added to corticosteroid therapy for the treatment of acute graft-versus-host disease. Biol Blood Marrow Transplant 15 : 804-811, 2009
43 Osiris Therapeutics Announces Preliminary Results for Prochymal Phase III GvHD Trials. http://investor.osiris.com/secfiling.cfm?

filingID=1104659-09-53523

44 Lee ST, Jang JH, Cheong JW, Kim JS, Maemg HY, *et al.* : Treatment of high-risk acute myelogenous leukaemia by myeloablative chemoradiotherapy followed by co-infusion of T cell-depleted haematopoietic stem cells and culture-expanded marrow mesenchymal stem cells from a related donor with one fully mismatched human leucocyte antigen haplotype. Br J Haematol 118 : 1128-1131, 2002

45 Lazarus HM, Koc ON, Devine SM, Curtin P, Maziarz RT, *et al.* : Cotransplantation of HLA-identical sibling culture-expanded mesenchymal stem cells and hematopoietic stem cells in hematologic malignancy patients. Biol Blood Marrow Transplant 11 : 389-398, 2005

46 Le Blanc K, Samuelsson H, Gustafsson B, Remberger M, Sundberg B, *et al.* : Transplantation of mesenchymal stem cells to enhance engraftment of hematopoietic stem cells. Leukemia 21 : 1733-1738, 2007

47 Ball LM, Bernardo ME, Roelofs H, Lankester A, Cometa A, *et al.* : Cotransplantation of *ex vivo* expanded mesenchymal stem cells accelerates lymphocyte recovery and may reduce the risk of graft failure in haploidentical hematopoietic stem-cell transplantation. Blood 110 : 2764-2767, 2007

48 Ning H, Yang F, Jiang M, Hu L, Feng K, *et al.* : The correlation between cotransplantation of mesenchymal stem cells and higher recurrence rate in hematologic malignancy patients : outcome of a pilot clinical study. Leukemia 22 : 593-599, 2008

49 Zhang X, Li JY, Cao K, Lu H, Hong M, *et al.* : Cotransplantation of HLA-identical mesenchymal stem cells and hematopoietic stem cells in Chinese patients with hematologic diseases. Int J Lab Hematol 32 : 256-264, 2010

50 Gonzalo-Daganzo R, Regidor C, Martín-Donaire T, Rico MA, Bautista G, *et al.* : Results of a pilot study on the use of third-party donor mesenchymal stromal cells in cord blood transplantation in adults. Cytotherapy 11 : 278-288, 2009

51 Zhou H, Guo M, Bian C, Sun Z, Yang Z, *et al.* : Efficacy of bone marrow-derived mesenchymal stem cells in the treatment for sclerodermatous chronic graft-versus-host disease : a clinical report of four patients. Biol Blood Marrow Transplant 16 : 403-412, 2010

52 Ringdén O, Uzunel M, Sundberg B, Lönnies L, Nava S, *et al.* : Tissue repair using allogeneic mesenchymal stem cells for hemorrhagic cystitis, pneumomediastinum and perforated colon. Leukemia 21 : 2271-2276, 2007

Altered Effector CD4$^+$ T Cell Function in IL-21R$^{-/-}$ CD4$^+$ T Cell-Mediated Graft-Versus-Host Disease

Iekuni Oh,* Katsutoshi Ozaki,* Akiko Meguro,* Keiko Hatanaka,* Masanori Kadowaki,† Haruko Matsu,* Raine Tatara,* Kazuya Sato,* Yoichiro Iwakura,‡ Susumu Nakae,§ Katsuko Sudo,¶ Takanori Teshima,† Warren J. Leonard,‖ and Keiya Ozawa*

We previously showed that transplantation with *IL-21R* gene-deficient splenocytes resulted in less severe graft-versus-host disease (GVHD) than was observed with wild type splenocytes. In this study, we sought to find mechanism(s) explaining this observation. Recipients of donor CD4$^+$ T cells lacking IL-21R exhibited diminished GVHD symptoms, with reduced inflammatory cell infiltration into the liver and intestine, leading to prolonged survival. After transplantation, CD4$^+$ T cell numbers in the spleen were reduced, and MLR and cytokine production by CD4$^+$ T cells were impaired. These results suggest that IL-21 might promote GVHD through enhanced production of effector CD4$^+$ T cells. Moreover, we found that CD25 depletion altered neither the impaired MLR in vitro nor the ameliorated GVHD symptoms in vivo. Thus, the attenuated GVHD might be caused by an impairment of effector T cell differentiation itself, rather than by an increase in regulatory T cells and suppression of effector T cells. *The Journal of Immunology*, 2010, 185: 1920–1926.

Interleukin-21 was discovered as a costimulatory cytokine for T cell proliferation and NK cell expansion in vitro (1, 2). IL-21 is produced by activated CD4 T cells (1), and its receptor is expressed on T, B, and NK cells (1, 3). It was also reported that IL-21 suppresses dendritic cell function (4) and increases hematopoietic progenitor cells (5). IL-21 is known to play critical roles in Ig production (6), whereas reports have differed regarding its contributions to Th1-, Th2-, and Th17-mediated effects and differentiation (6–15). IL-21 contributes to Th17 differentiation, but it may not be required for this process (7, 9, 14, 15). A relationship between IL-21 and autoimmune disease has been established. Overexpression of IL-21 induces inflammation, and in a systemic lupus erythematosus model mouse (the BXSB.6-Yaa$^+$/J) with high serum levels of IL-21 (16), the development of disease is abrogated when these mice are crossed to IL-21R knockout (KO) mice (17). In addition, autoimmune NOD mice do not develop diabetes in the absence of IL-21 signaling (18–20).

Graft-versus-host disease (GVHD) is a major complication following hematopoietic stem cell transplantation (21), sometimes with a fatal outcome. Previously, we showed that transplantation with *IL-21R* gene-disrupted splenocytes resulted in less severe GVHD than was seen with wild type (WT) splenocytes (22). We sought to elucidate the mechanism(s) for this observation; in this article, we demonstrate dysregulated effector function of activated CD4$^+$ T cells in IL-21R$^{-/-}$ mice.

Materials and Methods

Mice

IL-21R$^{-/-}$ and IL-17$^{-/-}$ mice were generated previously (6, 23). Both were on a C57BL/6 background. Male and female mice were used as donors. C57BL/6-DBA2-F1 male mice were purchased from Clea Japan (Tokyo, Japan). All mice used in experiments were 6–12 wk old. All mice were housed in a Jichi Medical University mouse facility, which is regulated by an intramural small animal committee, and were treated in accordance with university guidelines.

In vitro T cell stimulation and MLR

Cells were cultured in RPMI 1640 (Invitrogen, Carlsbad, CA) supplemented with 10% FCS (Sigma-Aldrich, St. Louis, MO), 2 mM L-glutamine (Invitrogen), 50 μM 2-ME (Sigma-Aldrich), 0.1 mg/ml streptomycin, and 100 U/ml penicillin G (Invitrogen). Nonspecific pan T cell stimulation was performed using anti-CD3/CD28 beads for 3 d, according to the manufacturer's instructions (Dynal Biotech, Oslo, Norway). Alloantigen-specific T cell stimulation was induced by cocultivation of CD4 T cells with 30 Gy-irradiated splenocytes from C57BL/6-DBA2-F1 mice for 4 d.

GVHD models

We used IL-21R$^{-/-}$ bone marrow (BM) to eliminate the effects of WT T cells in BM. We compared transplantations with IL-21R$^{-/-}$ CD4$^+$ T cells versus WT CD4$^+$ T cells. C57BL/6-DBA2-F1 mice were irradiated with 11 Gy and injected i.v. with 5×10^6 IL-21R$^{-/-}$ BM and 5×10^6 purified CD4$^+$ T cells from WT or IL-21R$^{-/-}$ mice. The cells were purified using CD4 microbeads and AutoMACS (Miltenyi Biotec, Tokyo, Japan); the purity was >80–90%.

Pathological analysis

Two weeks after transplantation, mice were sacrificed; liver, skin, and intestine were subjected to formalin fixation, paraffin embedding, excision, and H&E staining. Photographs were taken with an Olympus BX51 microscope at ×400 magnification.

Flow cytometric analysis

Fc-block (BD Biosciences, San Jose, CA) was used to prevent nonspecific Ab binding to Fc receptors. Abs to CD4 (RM4-5), CD8 (Ly-2), CD25

*Division of Hematology, Department of Medicine, Jichi Medical University, Tochigi; †Department of Medicine and Biosystemic Science, Kyushu University Graduate School of Medical Science, Fukuoka; ‡Center for Experimental Medicine and §Frontier Research Initiative, Institute of Medical Science, University of Tokyo; ¶Animal Research Center, Tokyo Medical University, Tokyo, Japan; and ‖Laboratory of Molecular Immunology, National Heart, Lung, and Blood Institute, National Institutes of Health, Bethesda, MD 20892

Received for publication July 14, 2009. Accepted for publication May 10, 2010.

This work was supported in part by grants from the Ministry of Health, Labor and Welfare of Japan; by grants-in-aid for Scientific Research from the Ministry of Education, Culture, Sports, Science and Technology of Japan; and by the Intramural Research Program of the National Heart, Lung and Blood Institute, National Institutes of Health, Bethesda, MD.

Address correspondence and reprint requests to Dr. Katsutoshi Ozaki, Division of Hematology, Department of Medicine, Jichi Medical University, 3311-1 Yakushiji, Shimotsuke-shi, Tochigi 329-0498, Japan. E-mail address: ozakikat@jichi.ac.jp

The online version of this article contains supplemental material.

Abbreviations used in this paper: BM, bone marrow; GVHD, graft-versus-host disease; KO, knockout; Treg, regulatory T; WT, wild type.

www.jimmunol.org/cgi/doi/10.4049/jimmunol.0902217

(7D4), H-2^b (AF6-88.5), H-2^d (SF1-1.1), IFN-γ (XMG1.2), and TNF-α (MP6-XT22) were purchased from BD Biosciences, and anti-Foxp3 (FJK-16a) was from eBioscience (San Diego, CA). Intracellular staining was performed with a Cytofx/Cytoperm kit (BD Biosciences), according to the manufacturer's instructions. Cells were stimulated with anti-mouse CD3/CD28 beads for 5 h in the presence of GolgiStop (BD Biosciences). The stimulation was omitted for Foxp3 intracellular staining. An LSR flow cytometer (BD Biosciences) was used for data collection, and data were analyzed using CellQuest software (BD Biosciences).

ELISA

ELISA kits for IL-2, IL-4, and IFN-γ were from BD Biosciences, and ELISA kits for IL-21, IL-17, TNF-α, and TGF-β1 were from R&D Systems (Minneapolis, MN). Concentrations were determined according to the manufacturer's instructions.

CD25 depletion in vitro and in vivo

In vitro purification of CD4$^+$ T cells and depletion of the CD25$^+$CD4$^+$ subpopulation were performed by cell sorting using a FACSAria (BD Biosciences), which yielded highly pure populations (>98%). In vivo CD25 depletion was performed by injecting anti-CD25 Ab, as described previously (24, 25). Briefly, a hybridoma producing anti-CD25 Ab (PC61; American Type Culture Collection, Manassas, VA) was cultured in serum-free medium (Protein-Free Hybridoma Medium-II from Invitrogen), and the Ab was purified from supernatant by ammonium sulfate precipitation and a PD10 column (GE Healthcare, Buckinghamshire, U.K.). The purified product was quantified using the Bradford assay (Bio-Rad, Hercules, CA) at OD595, and 1 mg was injected i.p. weekly from day 0 for 3 wk. Control rat nonspecific IgG was purchased from Invitrogen.

Quantitative RT-PCR

At day 21 after bone marrow transplantation, CD25$^-$CD4$^+$ T cells were purified by cell sorting from recipients of WT or IL-21R$^{-/-}$ CD4$^+$ T cells; RNA was isolated (RNeasy, Qiagen, Valencia, CA), reverse transcribed using the SuperScript First-Strand Synthesis System for RT-PCR (Invitrogen), and PCR amplified using TaqMan Gene Expression Assay's primer for mouse Foxp3 (Mm00475156) and β-actin (Mm00607939) and an ABI Prism 7700 sequence detection System (Applied Biosystems, Foster City, CA).

Statistical analysis

Kaplan–Meier plots were used to compare survival rates. The log-rank test was used to evaluate p values. Statistical analyses were performed using Stat Mate ver. 6 (ATMS, Tokyo, Japan). The Student t test was used; all error bars in this study represent SD, unless otherwise specified.

Results

Purified CD4$^+$ T cell transplantation and pathological analysis

Decreased GVHD was observed when we transplanted IL-21R–deficient splenocytes compared with WT bulk splenocytes (22). Although we sought to find molecular mechanism(s) for the ameliorated GVHD, no clue was immediately evident from the transplantation experiments (22). Thus, in this study, we used purified CD4$^+$ T cells instead of bulk splenocytes in an effort to augment the differences observed. We used a well-known model of CD4$^+$ T cell-mediated GVHD (26), in which C57BL/6 mice were donors, and C57BL/6-DBA2-F1 mice were recipients. In this model, the difference between WT and IL-21R$^{-/-}$ cells seemed to be greater than in the previous experiments using bulk splenocytes (22). All recipients of WT CD4$^+$ T cells died within 55 d, whereas those receiving IL-21R$^{-/-}$ CD4$^+$ T cells survived during this time period (Fig. 1*A*). Moreover, recipients of IL-21R$^{-/-}$ CD4$^+$ T cells recovered from body weight loss by day 14, but those receiving WT CD4$^+$ T cells did not recover and continued to lose weight (Fig. 1*B*). In recipients of IL-21R$^{-/-}$ CD4$^+$ T cells, pathological analysis showed markedly reduced infiltration into the regions surrounding bile ducts and portal veins and into the interstitial region of small intestine compared with the infiltration observed in recipients of WT CD4$^+$ T cells (Fig. 2, *upper* and *middle panels*). Apoptotic bodies near the surface area of crypts in the small intestine were barely visible in recipients

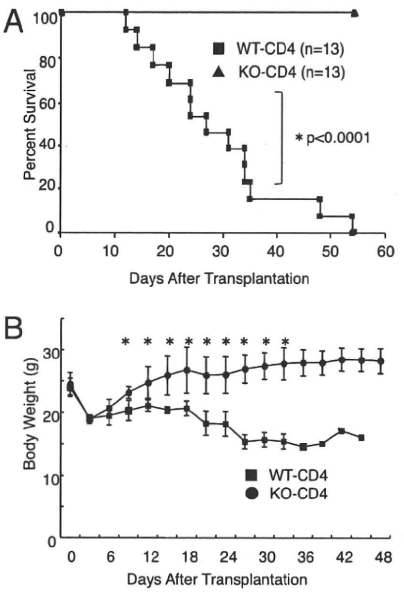

FIGURE 1. A role for IL-21 in CD4$^+$ T cell-mediated GVHD. *A*, Survival of recipients of WT and IL-21R$^{-/-}$ CD4$^+$ T cells. C57BL/6-DBA2-F1 mice were irradiated with 11 Gy and received 5 × 10^6 IL-21R$^{-/-}$ BM with 5 × 10^6 WT or IL-21R$^{-/-}$ CD4$^+$ T cells. Shown are combined data from two independent experiments. Thirteen recipients each for WT and IL-21R$^{-/-}$ CD4$^+$ T cells were analyzed. The log-rank test was used to calculate p values. *B*, Body weight after BM transplantation. Statistical significance was assessed with the Student t test.

of IL-21R$^{-/-}$ CD4$^+$ T cells, in contrast to recipients of WT CD4$^+$ T cells, in which apoptotic bodies were evident (Fig. 2, arrowheads in *middle panel*). No significant difference was observed in skin

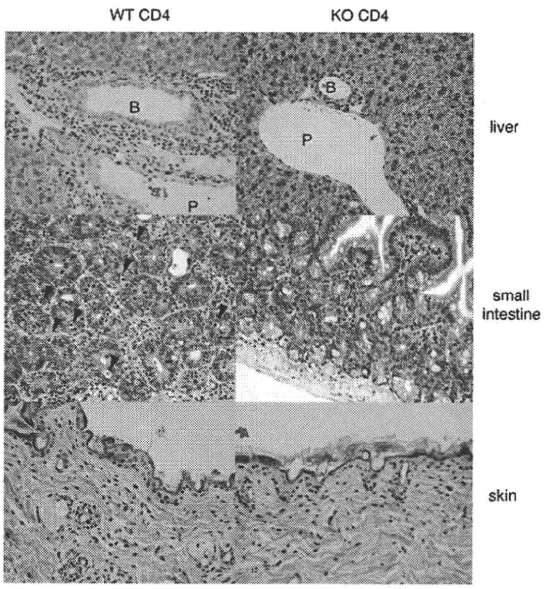

FIGURE 2. Pathological analysis of recipients. Liver, small intestine, and skin were stained with H&E (original magnification ×400). In recipients of WT CD4$^+$ T cells, cell infiltration is evident around the portal vein (P) and the bile duct (B) and into the interstitial region in small intestine. Arrowheads indicate apoptotic bodies near the surface of crypts. These changes were barely visible in recipients of IL-21R$^{-/-}$ CD4$^+$ T cells. Skin did not show any significant difference between recipients of WT and IL-21R$^{-/-}$ CD4$^+$ T cells. Shown is a representative result of six mice analyzed in each group. Only one recipient of IL-21R$^{-/-}$ CD4$^+$ T cells showed apoptotic bodies in the lumens of intestine and infiltration around the bile duct and portal vein, as was observed in the recipients of WT CD4$^+$ T cells.

pathology among recipients of WT CD4$^+$ and IL-21R$^{-/-}$ CD4$^+$ T cells. These results suggested that IL-21 might be essential for CD4-mediated GVHD, at least in this setting.

Normal cytokine production by splenocytes after transplantation is dependent on IL-21

The above observations suggested that IL-21–mediated donor CD4$^+$ T cell activation was involved in the exacerbation of GVHD. Because we could not find any significant difference in serum cytokine concentrations after transplantation (Supplemental Fig. 1), we assessed T cell differentiation by cytokine production in the presence of cellular stimulation. Interestingly, at days 14 and 21 after transplantation, bulk splenocytes from recipients of IL-21R$^{-/-}$ CD4$^+$ T cells exhibited defective cytokine production, with decreased levels of IFN-γ, TNF-α, and IL-4; in contrast, levels of IL-2, IL-17, and IL-21 were not significantly diminished (Fig. 3, *left panels*). Before transplantation, IL-21R$^{-/-}$ CD4$^+$ T cells did not show any significant defect in IFN-γ, IL-4, or TNF-α production (Fig. 3, *right panels*), suggesting that the defect was acquired after transplantation. This defect in effector T cell function might represent a mechanism for the difference in the development of GVHD by mice receiving WT versus IL-21R$^{-/-}$ CD4$^+$ T cells.

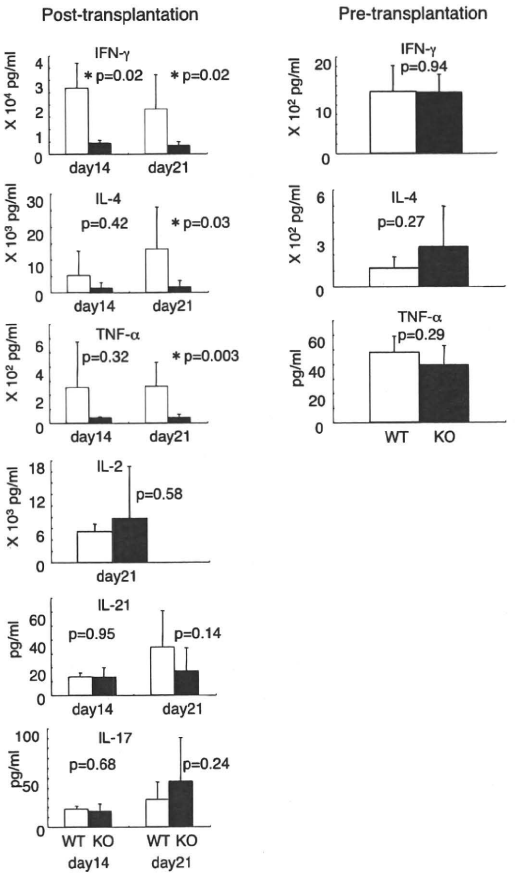

FIGURE 3. Cytokine production by bulk splenocytes before and after CD4$^+$ T cell transplantation. At days 14 and 21 after transplantation, splenocytes (5×10^5) were taken and stimulated with anti-CD3/CD28 Abs for 18 h. Concentrations of cytokines in the supernatants were determined by ELISA. Twelve or 13 recipients of WT CD4$^+$ T cells and 10 recipients of IL-21R$^{-/-}$ CD4$^+$ T cells were analyzed. Prior to transplantation, five WT and eight IL-21R$^{-/-}$ mice were analyzed. At days 14–21 after transplantation, the proportion of donor cells in the spleen was >95%. The Student *t* test was used to calculate *p* values. *Statistical significance ($p < 0.05$).

CD4$^+$ T cells were responsible for the low production of cytokines

To elucidate the basis for diminished cytokine production, we examined the number of donor CD4$^+$ T cells in the spleen at days 14–21 after transplantation. The number of donor H-2K^d$^-$CD4$^+$ T cells was significantly lower in recipients of IL-21R$^{-/-}$ CD4$^+$ T cells than in recipients of WT CD4$^+$ T cells (Fig. 4*A*; $p = 0.03$, Welch *t* test; $n = 15$ versus 12), although the ranges overlapped. Because it is thought that donor T cells proliferate in secondary lymphoid organs, such as the spleen, and then infiltrate into target organs (27), the reduced number of CD4$^+$ T cells in the spleen is consistent with the reduced infiltration into the liver and small intestine, as shown above (Fig. 2). To identify the cells responsible for defective cytokine production, we performed intracellular staining and ELISA with purified CD4$^+$ T cells. After anti-CD3/CD28 stimulation, the proportion of IFN-γ$^+$ and TNF-α$^+$ cells in splenic CD4$^+$ T cells was lower in recipients of IL-21R$^{-/-}$ CD4$^+$ T cells than in those receiving WT CD4$^+$ T cells (Fig. 4*B*). Moreover, posttransplantation, the levels

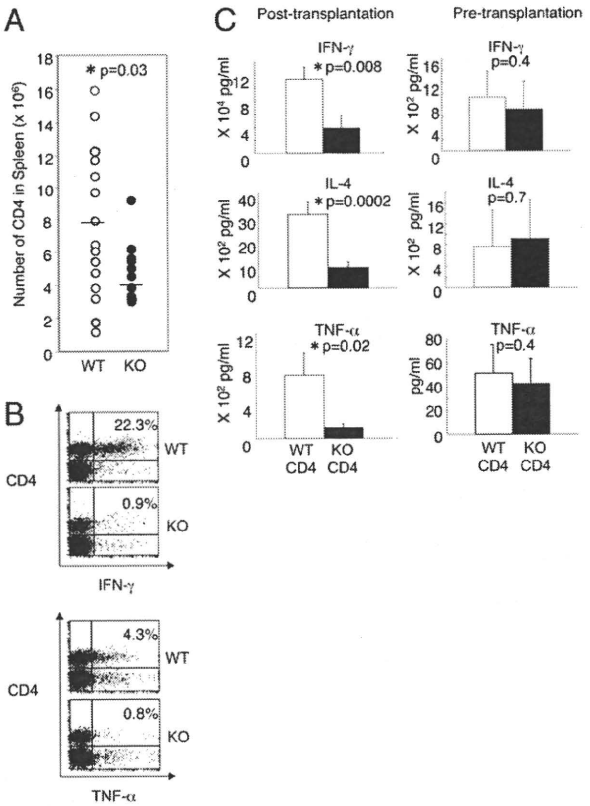

FIGURE 4. Cytokine production by splenic CD4$^+$ T cells before and after transplantation. *A*, Absolute number of donor H-2K^d$^-$CD4$^+$ T cells in the spleen. The number of donor CD4$^+$ T cells was determined by multiplying the number of splenocytes by the percentage of H-2K^d$^-$CD4$^+$ T cells. Each dot depicts the number of donor CD4$^+$ T cells in a mouse. Horizontal lines indicate the average. Fifteen recipients of WT CD4$^+$ T cells and 12 recipients of IL-21R$^{-/-}$ CD4$^+$ T cells were assessed. *B*, Intracellular staining of splenocytes after anti-CD3/CD28 stimulation. Splenocytes (1×10^6) were stimulated with anti-CD3/CD28 Abs for 5–6 h and stained with anti–IFN-γ or anti–TNF-α Ab in combination with anti-CD4 Ab. A total of three recipients in each group were analyzed, and a representative result is shown. *C*, Cytokine production by CD4$^+$ T cells in vitro. At days 14 or 21 after transplantation, splenic CD4$^+$ T cells (5×10^5) were purified and stimulated with anti-CD3/CD28 Abs for 18 h. Concentrations of cytokines in the supernatants were determined by ELISA. Twelve mice were analyzed in each group after transplantation. Five or six WT and eight or nine IL-21R$^{-/-}$ mice were analyzed before transplantation. *Statistical significance ($p < 0.05$).

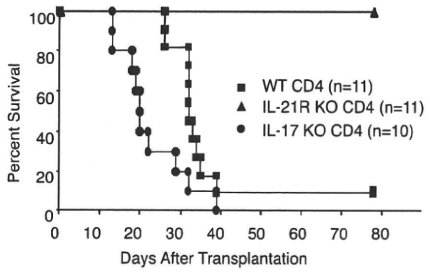

FIGURE 5. IL-17$^{-/-}$ CD4$^+$ T cells induced lethal GVHD. Survival of recipients of WT, IL-21R$^{-/-}$ (IL-21R KO), or IL-17$^{-/-}$ (IL-17 KO) CD4$^+$ T cells. Lethally irradiated (11 Gy) C57BL/6-DBA2-F1 mice were transplanted with 5×10^6 IL-21R KO BM and 5×10^6 WT, IL-21R KO, or IL-17 KO CD4$^+$ T cells. The data represent the combined results of two independent experiments.

of IFN-γ, TNF-α, and IL-4 production were significantly diminished with splenic-purified CD4$^+$ T cells from recipients of IL-21R$^{-/-}$ CD4$^+$ T cells compared with those receiving WT CD4$^+$ T cells (Fig. 4*C*, *left panels*). Before transplantation, IL-21R$^{-/-}$ CD4$^+$ T cells did not show any defect in IFN-γ, TNF-α, and IL-4 production (Fig. 4*C*, *right panels*).

IL-17 production and GVHD induced by IL-17$^{-/-}$ CD4$^+$ T cells

Although IL-21 is not essential for Th17 differentiation, IL-21 can promote it. To evaluate the effect of IL-21$^{-/-}$ CD4$^+$ T cell transplantation on IL-17 production, we measured IL-17 after transplantation. As shown in Fig 3, *bottom left panel*, bulk splenocytes from recipients of IL-21R$^{-/-}$ CD4$^+$ T cells produced comparable amounts of IL-17 at days 14 and 21 after transplantation compared with mice receiving WT CD4$^+$ T cells. Moreover, we found that IL-17$^{-/-}$ CD4$^+$ T cells induced lethal GVHD analogous to WT CD4$^+$ T cells (if anything, death occurred earlier), suggesting that IL-17 is dispensable for this process, in contrast to the essential role of IL-21, as reflected by the survival of mice receiving IL-21R$^{-/-}$ CD4$^+$ T cells (Fig. 5).

Regulatory T cell number in spleen

We next determined the serum concentration of the major immunosuppressive cytokine, TGF-β1, at days 6–21 after transplantation. We found an increase in TGF-β1 only after transplantation (Fig. 6*A*; $p = 0.0003$ at day 14; $p = 0.01$ at day 21, Student t test). In splenocytes from recipients of IL-21R$^{-/-}$ CD4$^+$ T cells, the production of TGF-β1 and IL-10 by in vitro T cell stimulation was not upregulated; in fact, it tended to be diminished (Supplemental Fig. 2), suggesting that the increase in serum TGF-β1 might be due to cells other than T cells. Because naive T cells can differentiate into regulatory T (Treg) cells in the presence of TGF-β1 (28), and it was reported that IL-21$^{-/-}$ T cells were predisposed to differentiate into Treg cells (8), we also investigated whether more Treg cells were induced in recipients of IL-21R$^{-/-}$ CD4$^+$ T cells. The proportion

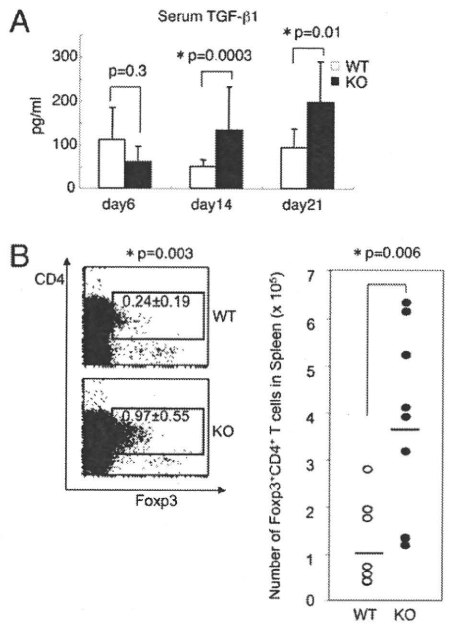

FIGURE 6. Increase in splenic Treg cells. *A*, Upregulation of serum TGF-β1. Serum TGF-β1 concentrations at the indicated day after transplantation were determined by ELISA. Three samples from recipients of WT CD4$^+$ T cells and 4 samples from recipients of IL-21R$^{-/-}$ CD4$^+$ T cells at day 6, 23 samples from recipients of WT CD4$^+$ T cells and 25 samples from recipients of IL-21R$^{-/-}$ CD4$^+$ T cells at day 14, and 8 samples from recipients of WT CD4$^+$ T cells and 7 samples from recipients of IL-21R$^{-/-}$ CD4$^+$ T cells at day 21 were analyzed. *Statistical significance ($p < 0.05$). *B*, The percentage and absolute number of splenic Foxp3$^+$CD4$^+$ regulatory T cells at day 14 after transplantation. The left panel shows a representative flow cytometric result from eight or nine similar samples. The right panel indicates the number of all samples; the averages are indicated by the horizontal lines.

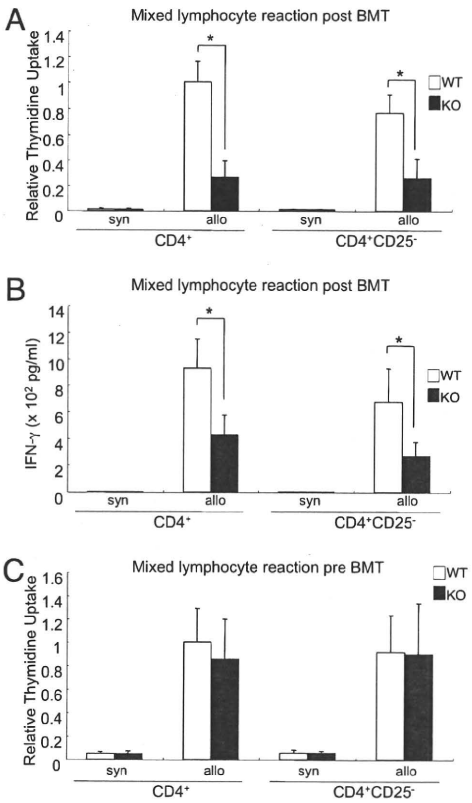

FIGURE 7. An impaired CD4 alloreaction is not dependent on CD25$^+$ CD4$^+$ T cells. CD4 alloreaction in vitro was impaired after transplantation, and this impairment was not restored by CD25$^+$ T cell depletion. *A*, At day 14 after transplantation, 1×10^5 sorter-purified splenic CD4$^+$ or CD25$^-$ CD4$^+$ T cells (>98% purity) were cultured with 4×10^5 irradiated allogeneic C57BL/6-DBA2-F1 splenocytes for 4 d. The cells were pulsed with 1 μCi of [^{3}H]thymidine for the last 24 h. Relative thymidine uptake to the value of WT CD4$^+$ T cells is depicted. *B*, Culture was the same as in *A*, but IFN-γ concentrations in the supernatants were determined by ELISA. *C*, Sorter-purified splenic CD4$^+$ or CD25$^-$CD4$^+$ cells from nontransplanted mice were cultured with irradiated allogeneic C57BL/6-DBA2-F1 splenocytes. Relative thymidine uptake to the number of WT CD4$^+$ T cells is depicted. *$p < 0.05$.

of splenic Foxp3$^+$CD4$^+$ Treg phenotype cells in recipients of IL-21R$^{-/-}$ CD4$^+$ T cells was higher than in recipients of WT CD4$^+$ T cells, but the total percentage was still only ~1% (Fig. 6*B*, *left panel*). The absolute number was ~4-fold higher, but the actual number was only ~4 × 10^5 of the total number of splenocytes (~4 × 10^7) (Fig. 6*B*, *right panel*). In contrast to posttransplantation, pretransplantation splenocytes from IL-21R$^{-/-}$ mice did not show an increase in Foxp3$^+$CD4$^+$ T cells compared with cells from WT mice (Supplemental Fig. 3), suggesting that the increased Treg cell after transplantation was an induced Treg cell during GVHD reaction. For that reason, we did not deplete CD25$^+$ cells prior to transplantation.

CD25 depletion did not restore the suppressed alloreaction in vitro and did not exacerbate the ameliorated GVHD

To investigate the importance of Treg cells in diminishing GVHD, we performed an MLR, which corresponds to alloreaction in vitro, with or without CD25$^+$CD4$^+$ T cells. Because Foxp3 is an intracellular protein, and Foxp3 staining cannot be used to purify or deplete Treg cells, anti-CD25 Ab is widely used for this purpose (9, 29–32). The impaired MLR of IL-21R$^{-/-}$ CD4$^+$ T cells after transplantation was not restored by CD25 depletion (Fig. 7*A*), nor was the impaired IFN-γ production by IL-21R$^{-/-}$CD4$^+$ T cells in an MLR (Fig. 7*B*). Moreover, analogous to cytokine production by anti-CD3/CD28 stimulation (Fig. 3), IL-21R$^{-/-}$ CD4$^+$ T cells before transplantation were not defective for alloreaction (Fig. 7*C*).

Consistent with the in vitro experiments above, CD25$^+$ depletion in vivo did not alter the severity of GVHD in recipients of IL-21R$^{-/-}$ CD4$^+$ T cells, without altering the body weight loss and survival (Fig. 8*A*, 8*B*). In contrast, the severity of GVHD in recipients of WT CD4$^+$ T cells seemed to be slightly diminished by CD25$^+$ depletion (Fig. 8*A*, 8*B*). In this condition, as previously reported (30), the depletion efficacy of CD25$^+$CD4$^+$ T cells was >95% and that of Foxp3$^+$CD4$^+$ T cells was ≥50% (Fig. 8*C*, *upper* and *lower panels*). Interestingly, Foxp3 expression was higher in CD25$^-$CD4$^+$ T cells from recipients of IL-21R$^{-/-}$ CD4$^+$ T cells than from recipients of WT CD4$^+$ T cells (Fig. 8*D*). Together with the results in vitro (Fig. 7), this suggests a relationship between the unresponsiveness of CD25$^-$CD4$^+$ T cells and greater expression of Foxp3.

Discussion

In this article, we reported evidence indicating that IL-21 is critical for the pathogenesis of CD4$^+$ T cell-mediated GVHD, at least in part because of its effects on CD4 differentiation. In this study, we focused on CD4$^+$ T cell-mediated GVHD; a role for IL-21 in CD8$^+$ T cell-mediated GVHD remains to be investigated.

We found a profound defect in T cell effector function only after transplantation, although serum cytokine concentrations showed no obvious difference. According to these results, T cell differentiation into Th1 and Th2 cells seemed to be altered in the absence of IL-21 during GVHD. Cytokines are believed to have positive and negative roles in GVHD. For example, although T cells from IFN-γ–deficient mice resulted in more severe GVHD (33–35), T cells from Stat4 (Th1)-deficient mice resulted in less severe GVHD than did T cells from WT mice with less severe colitis (36). In contrast to IFN-γ$^{-/-}$ T cells, T cells from IL-4–deficient mice induced less severe GVHD (34); analogously, T cells from Stat6 (Th2)-deficient mice induced less severe GVHD than did those from WT mice (36). T cells from TNF-α–deficient mice developed less severe GVHD, with less severe colitis (37). Our data suggest a strong correlation between the defect in effector function in recipients of IL-21R$^{-/-}$ CD4$^+$ T cells and the attenuated phenotype of GVHD, indicating a role for IL-21 in this process.

IL-21, as well as IL-6, induces Th17 differentiation in the presence of TGF-β, suggesting a possible involvement of IL-17 in

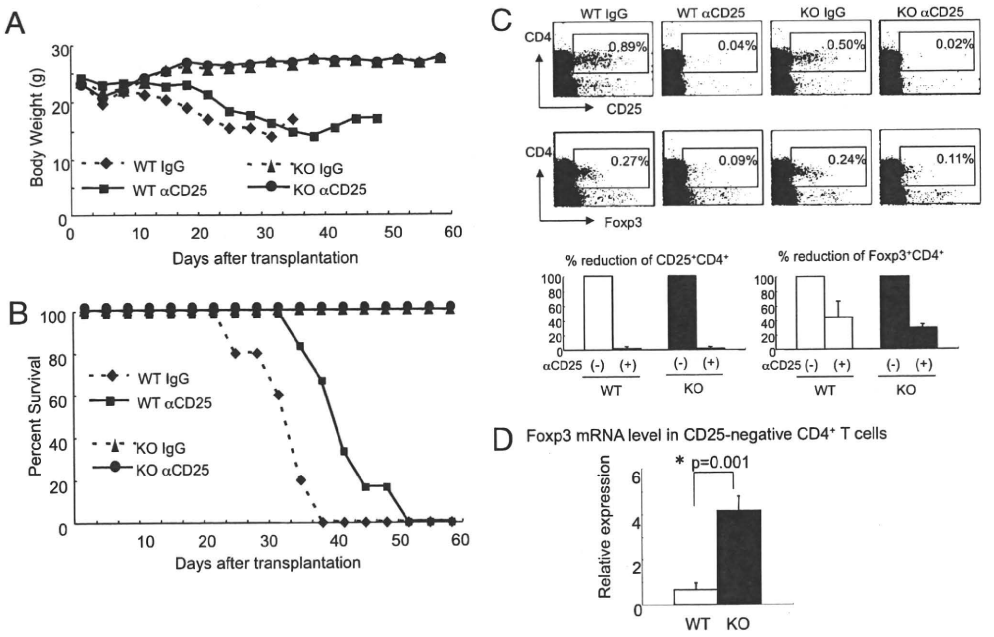

FIGURE 8. The ameliorated GVHD induced by IL-21R$^{-/-}$ CD4$^+$ T cells is not dependent on CD25$^+$CD4$^+$ T cells. The ameliorated GVHD induced by IL-21R$^{-/-}$ CD4$^+$ T cells was not exacerbated by depletion of CD25$^+$CD4$^+$ T cells. Body weight (*A*) and survival (*B*) of recipients are shown. Comparisons of recipients of WT CD4$^+$ T cells and IL-21R$^{-/-}$ CD4$^+$ T cells and additional comparisons with and without anti-CD25 Ab treatment were performed. Nonspecific rat IgG was used as the control Ab. *C*, Splenic CD25$^+$CD4$^+$ T cells and splenic Foxp3$^+$CD4$^+$ T cells at day 14 after transplantation with or without anti-CD25 Ab treatment were analyzed by flow cytometry (*upper two rows*). The lower panels indicate the mean reduction in the percentage of CD25$^+$CD4$^+$ and Foxp3$^+$CD4$^+$ cells from three similar results. *D*, Foxp3 mRNA level in CD25$^-$CD4$^+$ T cells at day 21 after transplantation. Cell sorter-purified CD25$^-$CD4$^+$ T cells were subjected to mRNA purification, reverse-transcriptase treatment, and TaqMan quantitative PCR. Relative value to β-actin is denoted.

the phenotype we observed. However, our results with IL-17$^{-/-}$ CD4$^+$ T cells demonstrated that IL-17 was dispensable for CD4$^+$ T cell-mediated GVHD, indicating that the attenuated GVHD in recipients of IL-21R$^{-/-}$ CD4$^+$ T cells was not due to an IL-17–related defect. During the preparation of this manuscript, a role for IL-17 in GVHD was reported (38–40). These reports varied, but one suggested that the lack of IL-17 promotes GVHD (38). Another report suggested that IL-17$^{-/-}$ CD4$^+$ T cells can ameliorate GVHD only at the early stages, which suggested a promoting effect for IL-17 at an early stage of GVHD (39). The third report suggested that ex vivo-differentiated Th17 cells induced skin and lung GVHD (40). Thus, the role of IL-17 may be complex and dependent on the specific experimental conditions.

Because there are reciprocal relationships between Th1/Th2 and Treg cell differentiation (41–43) and between IL-21 and Treg cell differentiation (8), we investigated the level of Treg cells in the spleens of recipients. Foxp3$^+$CD4$^+$ T cells were increased in percentage and absolute number but still represented only ~1% of splenocytes. Regarding the relationship between the defective effector T cell function and the increased number of Treg cells, it is possible that increased Treg cells suppress functional effector T cells. Alternatively, it is possible that effector differentiation itself is defective, and the resulting effector T cells cannot respond to alloantigen, analogous to the situation in T cell anergy, and that the increased Treg cell number is also a result of a dysregulated differentiation. Our results might be more consistent with the latter possibility, given that Treg cell depletion by anti-CD25 treatment did not alter the results in vitro and in vivo, although the efficiency of depletion of Foxp3$^+$CD4$^+$ T cells in vivo was incomplete. It is also conceivable that the upregulation of Foxp3 in CD25$^-$CD4$^+$ T cells (which would not be removed by CD25$^+$ depletion) in the absence of IL-21 signaling might result in unresponsiveness or poor responsiveness of effector T cells and that more than one mechanism can contribute to the attenuated GVHD.

Disclosures

K. Ozaki and W.J.L. are inventors on patents and patent applications related to IL-21.

References

1. Parrish-Novak, J., S. R. Dillon, A. Nelson, A. Hammond, C. Sprecher, J. A. Gross, J. Johnston, K. Madden, W. Xu, J. West, et al. 2000. Interleukin 21 and its receptor are involved in NK cell expansion and regulation of lymphocyte function. *Nature* 408: 57–63.
2. Spolski, R., and W. J. Leonard. 2008. Interleukin-21: basic biology and implications for cancer and autoimmunity. *Annu. Rev. Immunol.* 26: 57–79.
3. Ozaki, K., K. Kikly, D. Michalovich, P. R. Young, and W. J. Leonard. 2000. Cloning of a type I cytokine receptor most related to the IL-2 receptor beta chain. *Proc. Natl. Acad. Sci. USA* 97: 11439–11444.
4. Brandt, K., S. Bulfone-Paus, D. C. Foster, and R. Rückert. 2003. Interleukin-21 inhibits dendritic cell activation and maturation. *Blood* 102: 4090–4098.
5. Ozaki, K., A. Hishiya, K. Hatanaka, H. Nakajima, G. Wang, P. Hwu, T. Kitamura, K. Ozawa, W. J. Leonard, and T. Nosaka. 2006. Overexpression of interleukin 21 induces expansion of hematopoietic progenitor cells. *Int. J. Hematol.* 84: 224–230.
6. Ozaki, K., R. Spolski, C. G. Feng, C. F. Qi, J. Cheng, A. Sher, H. C. Morse, 3rd, C. Liu, P. L. Schwartzberg, and W. J. Leonard. 2002. A critical role for IL-21 in regulating immunoglobulin production. *Science* 298: 1630–1634.
7. Zhou, L., I. I. Ivanov, R. Spolski, R. Min, K. Shenderov, T. Egawa, D. E. Levy, W. J. Leonard, and D. R. Littman. 2007. IL-6 programs T(H)-17 cell differentiation by promoting sequential engagement of the IL-21 and IL-23 pathways. *Nat. Immunol.* 8: 967–974.
8. Nurieva, R., X. O. Yang, G. Martinez, Y. Zhang, A. D. Panopoulos, L. Ma, K. Schluns, Q. Tian, S. S. Watowich, A. M. Jetten, and C. Dong. 2007. Essential autocrine regulation by IL-21 in the generation of inflammatory T cells. *Nature* 448: 480–483.
9. Korn, T., E. Bettelli, W. Gao, A. Awasthi, A. Jäger, T. B. Strom, M. Oukka, and V. K. Kuchroo. 2007. IL-21 initiates an alternative pathway to induce proinflammatory T(H)17 cells. *Nature* 448: 484–487.
10. Wurster, A. L., V. L. Rodgers, A. R. Satoskar, M. J. Whitters, D. A. Young, M. Collins, and M. J. Grusby. 2002. Interleukin 21 is a T helper (Th) cell 2 cytokine that specifically inhibits the differentiation of naive Th cells into interferon gamma-producing Th1 cells. *J. Exp. Med.* 196: 969–977.
11. Pesce, J., M. Kaviratne, T. R. Ramalingam, R. W. Thompson, J. F. Urban, Jr., A. W. Cheever, D. A. Young, M. Collins, M. J. Grusby, and T. A. Wynn. 2006. The IL-21 receptor augments Th2 effector function and alternative macrophage activation. *J. Clin. Invest.* 116: 2044–2055.
12. Fröhlich, A., B. J. Marsland, I. Sonderegger, M. Kurrer, M. R. Hodge, N. L. Harris, and M. Kopf. 2007. IL-21 receptor signaling is integral to the development of Th2 effector responses in vivo. *Blood* 109: 2023–2031.
13. Strengell, M., T. Sareneva, D. Foster, I. Julkunen, and S. Matikainen. 2002. IL-21 up-regulates the expression of genes associated with innate immunity and Th1 response. *J. Immunol.* 169: 3600–3605.
14. Coquet, J. M., S. Chakravarti, M. J. Smyth, and D. I. Godfrey. 2008. Cutting edge: IL-21 is not essential for Th17 differentiation or experimental autoimmune encephalomyelitis. *J. Immunol.* 180: 7097–7101.
15. Sonderegger, I., J. Kisielow, R. Meier, C. King, and M. Kopf. 2008. IL-21 and IL-21R are not required for development of Th17 cells and autoimmunity in vivo. *Eur. J. Immunol.* 38: 1833–1838.
16. Ozaki, K., R. Spolski, R. Ettinger, H. P. Kim, G. Wang, C. F. Qi, P. Hwu, D. J. Shaffer, S. Akilesh, D. C. Roopenian, et al. 2004. Regulation of B cell differentiation and plasma cell generation by IL-21, a novel inducer of Blimp-1 and Bcl-6. *J. Immunol.* 173: 5361–5371.
17. Bubier, J. A., T. J. Sproule, O. Foreman, R. Spolski, D. J. Shaffer. H. C. Morse 3rd, W. J. Leonard, and D. C. Roopenian. 2009. A critical role for IL-21 receptor signaling in the pathogenesis of systemic lupus erythematosus in BXSB- Yaa mice. *Proc. Natl. Acad. Sci. U S A* 106: 1518–1523.
18. King, C., A. Ilic, K. Koelsch, and N. Sarvetnick. 2004. Homeostatic expansion of T cells during immune insufficiency generates autoimmunity. *Cell* 117: 265–277.
19. Spolski, R., M. Kashyap, C. Robinson, Z. Yu, and W. J. Leonard. 2008. IL-21 signaling is critical for the development of type I diabetes in the NOD mouse. *Proc. Natl. Acad. Sci. USA* 105: 14028–14033.
20. Sutherland, A. P., T. Van Belle, A. L. Wurster, A. Suto, M. Michaud, D. Zhang, M. J. Grusby, and M. von Herrath. 2009. Interleukin-21 is required for the development of type 1 diabetes in NOD mice. *Diabetes* 58: 1144–1155.
21. Shlomchik, W. D. 2007. Graft-versus-host disease. *Nat. Rev. Immunol.* 7: 340–352.
22. Meguro, A., K. Ozaki, I. Oh, K. Hatanaka, and H. Matsu, RTatara, K. Sato, W. J. Leonard, and K. Ozawa. 2010. IL-21 is critical for GVHD in a mouse model. *Bone Marrow Transplant.* 45: 723–729.
23. Nakae, S., Y. Komiyama, A. Nambu, K. Sudo, M. Iwase, I. Homma, K. Sekikawa, M. Asano, and Y. Iwakura. 2002. Antigen-specific T cell sensitization is impaired in IL-17-deficient mice, causing suppression of allergic cellular and humoral responses. *Immunity* 17: 375–387.
24. Sakoda, Y., D. Hashimoto, S. Asakura, K. Takeuchi, M. Harada, M. Tanimoto, and T. Teshima. 2007. Donor-derived thymic-dependent T cells cause chronic graft-versus-host disease. *Blood* 109: 1756–1764.
25. Aoyama, K., M. Koyama, K. Matsuoka, D. Hashimoto, T. Ichinohe, M. Harada, K. Akashi, M. Tanimoto, and T. Teshima. 2009. Improved outcome of allogeneic bone marrow transplantation due to breastfeeding-induced tolerance to maternal antigens. *Blood* 113: 1829–1833.
26. Teshima, T., G. R. Hill, L. Pan, Y. S. Brinson, M. R. van den Brink, K. R. Cooke, and J. L. Ferrara. 1999. IL-11 separates graft-versus-leukemia effects from graft-versus-host disease after bone marrow transplantation. *J. Clin. Invest.* 104: 317–325.
27. Beilhack, A., S. Schulz, J. Baker, G. F. Beilhack, C. B. Wieland, E. I. Herman, E. M. Baker, Y. A. Cao, C. H. Contag, and R. S. Negrin. 2005. In vivo analyses of early events in acute graft-versus-host disease reveal sequential infiltration of T-cell subsets. *Blood* 106: 1113–1122.
28. Sakaguchi, S., T. Yamaguchi, T. Nomura, and M. Ono. 2008. Regulatory T cells and immune tolerance. *Cell* 133: 775–787.
29. Sakaguchi, S., N. Sakaguchi, M. Asano, M. Itoh, and M. Toda. 1995. Immunologic self-tolerance maintained by activated T cells expressing IL-2 receptor alpha-chains (CD25). Breakdown of a single mechanism of self-tolerance causes various autoimmune diseases. *J. Immunol.* 155: 1151–1164.
30. Liesz, A., E. Suri-Payer, C. Veltkamp, H. Doerr, C. Sommer, S. Rivest, T. Giese, and R. Veltkamp. 2009. Regulatory T cells are key cerebroprotective immunomodulators in acute experimental stroke. *Nat. Med.* 15: 192–199.
31. Fujita, S., Y. Sato, K. Sato, K. Eizumi, T. Fukaya, M. Kubo, N. Yamashita, and K. Sato. 2007. Regulatory dendritic cells protect against cutaneous chronic graft-versus-host disease mediated through CD4+CD25+Foxp3+ regulatory T cells. *Blood* 110: 3793–3803.
32. Radojcic, V., M. A. Pletneva, H. R. Yen, S. Ivcevic, A. Panoskaltsis-Mortari, A. C. Gilliam, C. G. Drake, B. R. Blazar, and L. Luznik. 2010. STAT3 signaling in CD4+ T cells is critical for the pathogenesis of chronic sclerodermatous graft-versus-host disease in a murine model. *J. Immunol.* 184: 764–774.
33. Yang, Y. G., B. R. Dey, J. J. Sergio, D. A. Pearson, and M. Sykes. 1998. Donor-derived interferon gamma is required for inhibition of acute graft-versus-host disease by interleukin 12. *J. Clin. Invest.* 102: 2126–2135.
34. Murphy, W. J., L. A. Welniak, D. D. Taub, R. H. Wiltrout, P. A. Taylor, D. A. Vallera, M. Kopf, H. Young, D. L. Longo, and B. R. Blazar. 1998. Differential effects of the absence of interferon-gamma and IL-4 in acute graft-versus-host disease after allogeneic bone marrow transplantation in mice. *J. Clin. Invest.* 102: 1742–1748.
35. Wang, H., W. Asavaroengchai, B. Y. Yeap, M. G. Wang, S. Wang, M. Sykes, and Y. G. Yang. 2009. Paradoxical effects of IFN-gamma in graft-versus-host disease reflect promotion of lymphohematopoietic graft-versus-host reactions and inhibition of epithelial tissue injury. *Blood* 113: 3612–3619.
36. Nikolic, B., S. Lee, R. T. Bronson, M. J. Grusby, and M. Sykes. 2000. Th1 and Th2 mediate acute graft-versus-host disease, each with distinct end-organ targets. *J. Clin. Invest.* 105: 1289–1298.

37. Schmaltz, C., O. Alpdogan, S. J. Muriglan, B. J. Kappel, J. A. Rotolo, E. T. Ricchetti, A. S. Greenberg, L. M. Willis, G. F. Murphy, J. M. Crawford, and M. R. van den Brink. 2003. Donor T cell-derived TNF is required for graft-versus-host disease and graft-versus-tumor activity after bone marrow transplantation. *Blood* 101: 2440–2445.
38. Yi, T., D. Zhao, C. L. Lin, C. Zhang, Y. Chen, I. Todorov, T. LeBon, F. Kandeel, S. Forman, and D. Zeng. 2008. Absence of donor Th17 leads to augmented Th1 differentiation and exacerbated acute graft-versus-host disease. *Blood* 112: 2101–2110.
39. Kappel, L. W., G. L. Goldberg, C. G. King, D. Y. Suh, O. M. Smith, C. Ligh, A. M. Holland, J. Grubin, N. M. Mark, C. Liu, et al. 2009. IL-17 contributes to CD4-mediated graft-versus-host disease. *Blood* 113: 945–952.
40. Carlson, M. J., M. L. West, J. M. Coghill, A. Panoskaltsis-Mortari, B. R. Blazar, and J. S. Serody. 2009. In vitro-differentiated TH17 cells mediate lethal acute graft-versus-host disease with severe cutaneous and pulmonary pathologic manifestations. *Blood* 113: 1365–1374.
41. Wei, J., O. Duramad, O. A. Perng, S. L. Reiner, Y. J. Liu, and F. X. Qin. 2007. Antagonistic nature of T helper 1/2 developmental programs in opposing peripheral induction of Foxp3+ regulatory T cells. *Proc. Natl. Acad. Sci. USA* 104: 18169–18174.
42. Mantel, P. Y., H. Kuipers, O. Boyman, C. Rhyner, N. Ouaked, B. Rückert, C. Karagiannidis, B. N. Lambrecht, R. W. Hendriks, R. Crameri, et al. 2007. GATA3-driven Th2 responses inhibit TGF-beta1-induced FOXP3 expression and the formation of regulatory T cells. *PLoS Biol.* 5: e329.
43. Hill, J. A., J. A. Hall, C. M. Sun, Q. Cai, N. Ghyselinck, P. Chambon, Y. Belkaid, D. Mathis, and C. Benoist. 2008. Retinoic acid enhances Foxp3 induction indirectly by relieving inhibition from CD4+CD44hi Cells. *Immunity* 29: 758–770.

Histone deacetylases are critical targets of bortezomib-induced cytotoxicity in multiple myeloma

Jiro Kikuchi,[1] Taeko Wada,[1] Rumi Shimizu,[1] Tohru Izumi,[2] Miyuki Akutsu,[2] Kanae Mitsunaga,[1] Kaoru Noborio-Hatano,[3] Masaharu Nobuyoshi,[3] Keiya Ozawa,[3] Yasuhiko Kano,[2] and Yusuke Furukawa[1,3]

[1]Division of Stem Cell Regulation, Center for Molecular Medicine, Jichi Medical University, Shimotsuke, Tochigi; [2]Division of Hematology, Tochigi Cancer Center, Utsunomiya, Tochigi; and [3]Division of Hematology, Department of Internal Medicine, Jichi Medical University, Shimotsuke, Tochigi, Japan

Bortezomib is now widely used for the treatment of multiple myeloma (MM); however, its action mechanisms are not fully understood. Despite the initial results, recent investigations have indicated that bortezomib does not inactivate nuclear factor-κB activity in MM cells, suggesting the presence of other critical pathways leading to cytotoxicity. In this study, we show that histone deacetylases (HDACs) are critical targets of bortezomib, which specifically down-regulated the expression of class I HDACs (HDAC1, HDAC2, and HDAC3) in MM cell lines and primary MM cells at the transcriptional level, accompanied by reciprocal histone hyperacetylation. Transcriptional repression of HDACs was mediated by caspase-8–dependent degradation of Sp1 protein, the most potent transactivator of class I HDAC genes. Short-interfering RNA-mediated knockdown of HDAC1 enhanced bortezomib-induced apoptosis and histone hyperacetylation, whereas HDAC1 overexpression inhibited them. HDAC1 overexpression conferred resistance to bortezomib in MM cells, and administration of the HDAC inhibitor romidepsin restored sensitivity to bortezomib in HDAC1-overexpressing cells both in vitro and in vivo. These results suggest that bortezomib targets HDACs via distinct mechanisms from conventional HDAC inhibitors. Our findings provide a novel molecular basis and rationale for the use of bortezomib in MM treatment. (*Blood.* 2010;116(3):406-417)

Introduction

Despite recent advances in treatment strategies using dose-intensified regimens and new molecular-targeted compounds, multiple myeloma (MM) remains incurable for most patients.[1] To improve their prognosis, the development of molecular-targeted therapy, which involves therapeutic agents with distinct mechanisms of action and high specificity, is highly anticipated. Inhibitors of histone deacetylases (HDACs) and proteasome are promising candidates for these agents, and their clinical efficacy has been reported.[2-4] Moreover, their combinations were proved to be additive in preclinical studies[5,6] and are presently the focus of clinical trials.[7]

Aberrant transcriptional repression of genes regulating cell growth and differentiation is a hallmark of cancer.[8] Recently, evidence has accumulated suggesting that altered activation of HDACs underlies transcriptional repression in malignancies.[9] HDACs are a family of enzymes that catalyze the removal of acetyl groups from core histones, resulting in chromatin compaction and transcriptional repression.[10] HDACs are divided into 5 groups: class I (HDAC1, HDAC2, HDAC3, and HDAC8), class IIa (HDAC4, HDAC5, HDAC7, and HDAC9), class IIb (HDAC6 and HDAC10), class III (SIRT family), and class IV (HDAC11). Class I HDACs are ubiquitously expressed and are generally involved in cell growth and differentiation,[11] whereas class II HDACs have a more restricted pattern of expression (skeletal muscle, heart, and brain) and act in association with tissue-specific transcription factors. In leukemic cells, fusion proteins such as PML/RARα and AML-1/ETO form a complex with HDACs with higher affinities than their normal counterparts, and aberrantly suppress the expression of genes required for cell differentiation and growth control, leading to the transformation of hematopoietic progenitor cells.[12,13] In addition, we have shown that class I HDACs are up-regulated in malignant melanoma and leukemias in association with histone hypoacetylation.[14,15] Similarly, the aberrant expression of HDACs may contribute to the uncontrolled growth of myeloma cells.

Given the role of HDACs in tumor cells, the use of small compounds that inhibit HDAC activity, collectively referred to as HDAC inhibitors, is expected to become a novel strategy for the treatment of cancer.[16] HDAC inhibitors are able to restore the expression of genes that are aberrantly suppressed in tumor cells, which may result in cell-cycle arrest, differentiation, and apoptosis.[17]

The proteasome inhibitor bortezomib (Velcade [Millennium Pharmaceuticals]; formerly known as PS-341) is now widely used for the treatment of MM.[3,4] Bortezomib is a reversible inhibitor of the 26S proteasome complex, which catalyzes ubiquitin-dependent protein degradation. Inhibition of this complex ultimately leads to modulation of the abundance and functions of many intracellular proteins, which may be associated with cytotoxic effects on malignant cells.[18] Recently, novel proteasome inhibitors, which target the ubiquitin-proteasome system in a manner distinct from bortezomib, have been developed and have shown strong activity in preclinical studies.[19,20] These new inhibitors are thought to be promising candidates for MM treatment.

Recent genome-wide approaches have revealed that nuclear factor-κB (NF-κB) is frequently activated in MM cells.[21,22] Because IκBα, which inactivates NF-κB, is a substrate of the

Submitted July 31, 2009; accepted February 23, 2010. Prepublished online as *Blood* First Edition paper, March 29, 2010; DOI 10.1182/blood-2009-07-235663.

An Inside *Blood* analysis of this article appears at the front of this issue.

The online version of this article contains a data supplement.

The publication costs of this article were defrayed in part by page charge payment. Therefore, and solely to indicate this fact, this article is hereby marked "advertisement" in accordance with 18 USC section 1734.

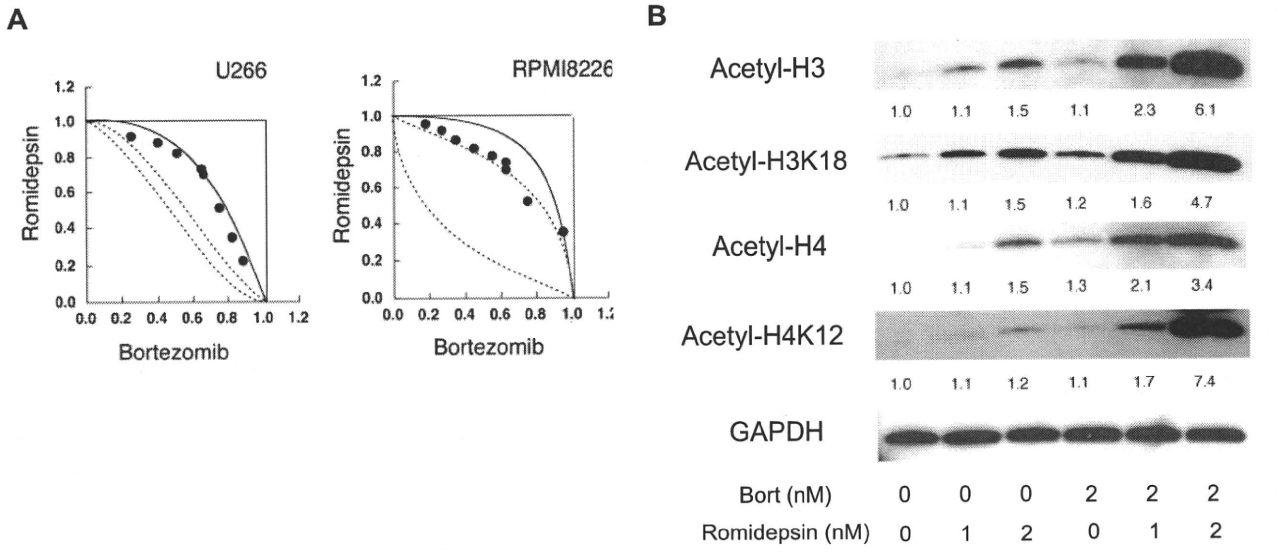

Figure 1. Synergistic effects of romidepsin and bortezomib on cell viability and histone acetylation. (A) Isobolograms of simultaneous exposure of U266 and RPMI8226 cells to bortezomib and romidepsin are shown. The concentrations that produced 80% growth inhibition are expressed as 1.0 on the ordinate and abscissa of isobolograms. The envelope of additivity, surrounded by solid and broken lines, is constructed from dose-response curves of bortezomib and romidepsin. When the data points of the drug combination fall within the area surrounded by the envelope of additivity, the combination is regarded as additive. When the data points fall to the left of the envelope, the drug combination is regarded as supra-additive (synergism). When the data points fall to the right of the envelope, the combination is regarded as antagonistic. The isobolograms shown are representative of at least 3 independent experiments. Each point represents the mean value of at least 3 independent experiments; the SEMs were less than 25% and were omitted. (B) U266 cells were cultured in the absence or presence of either romidepsin (Romidepsin), bortezomib (Bort), or both agents for 48 hours at the indicated doses. Whole-cell lysates were subjected to immunoblotting. The membranes were reprobed with anti-GAPDH antibody to serve as a loading control. The signal intensities of each band were quantified, normalized to those of the corresponding GAPDH, and shown as relative values setting untreated controls to 1.0. Data shown are representative of multiple independent experiments.

proteasome complex, the initial rationale for the use of bortezomib was the inhibition of NF-κB activity.[23] Despite several preclinical studies and clinical trials of MM,[3,4] the inhibition of NF-κB activity has not been demonstrated in bortezomib-treated MM cells. In addition, Hideshima et al[24] recently reported that bortezomib did not inactivate but rather activated the canonical NF-κB pathway in MM cells, suggesting that bortezomib-induced cytotoxicity could not be fully attributed to the inhibition of NF-κB activity. Taken together, there may be other critical pathways and target molecules of bortezomib that have not been fully investigated.

In this study, we found that bortezomib specifically down-regulated the expression of class I HDACs and induced histone hyperacetylation in MM cells. Gain- and loss-of-function analyses revealed that bortezomib-induced cytotoxicity depends on cellular HDAC activities both in vitro and in vivo. Based on these findings, we propose that HDACs are novel critical downstream targets of bortezomib. This finding may provide a novel molecular basis and rationale for the use of bortezomib in MM treatment.

Methods

Cells and cell culture

We used 3 bona fide human MM cell lines, KMS12-BM, RPMI8226, and U266, in this study.[25] These cell lines were purchased from the Health Science Research Resources Bank and maintained in RPMI 1640 medium (Sigma-Aldrich) supplemented with 10% heat-inactivated fetal calf serum (Sigma-Aldrich) and antibiotics. Primary CD138$^+$ MM cells were isolated from the bone marrow (BM) of patients at the time of diagnostic procedure using the magnetic-activated cell sorter (MACS) system (Miltenyi Biotec). Informed consent was obtained in accordance with the Declaration of Helsinki, and the protocol was approved by the institutional review board of Jichi Medical University.

Drugs

Bortezomib and romidepsin (formerly known as FK228 or depsipeptide) were obtained from Millennium Pharmaceuticals and Gloucester Pharmaceuticals, respectively. HDAC6-specific inhibitor tubacin and its inactive derivative niltubacin were provided by Dr Stuart L. Schreiber (Broad Institute of Harvard University and Massachusetts Institute of Technology). We used vincristine (Shionogi Co Ltd), doxorubicin (Meiji Co Ltd), and dexamethasone (Sigma-Aldrich) as conventional antimyeloma drugs. All drugs were dissolved in RPMI 1640 medium at appropriate concentrations and stored at −80°C until use.

Isobologram of Steel and Peckham

The cytotoxic interaction of bortezomib and romidepsin was evaluated at the point of IC_{80} by the isobologram of Steel and Peckham. IC_{80} was defined as the concentration of drugs that produced 80% inhibition of cell growth. The theoretical basis of the isobologram method has been previously described in detail.[26]

Assessment of cell death

Cells were washed with phosphate-buffered saline (PBS) and stained with allophycocyanin-conjugated annexin-V (annexin-V/APC; Biovision). Cell death/apoptosis was judged by annexin-V reactivity and BrdU/7-AAD double-staining using a FACSAria flow cytometer (Becton Dickinson) as described previously.[27]

Immunoblotting

Immunoblotting was carried out according to the standard method using the following antibodies: antiacetyl histone H3, antiacetyl histone H4 (Upstate Biotechnology/Millipore), antiacetyl histone H3–lysine18, antiacetyl histone H4–lysine12, antiacetyl–α-tubulin (Cell Signaling Technology), anti-HDAC1 (Sigma-Aldrich), anti-HDAC2 (MBL International), anti-HDAC3 (BD PharMingen), anti-Sp1, anti–MZF-1, and anti-GAPDH (Santa Cruz Biotechnology).[28]

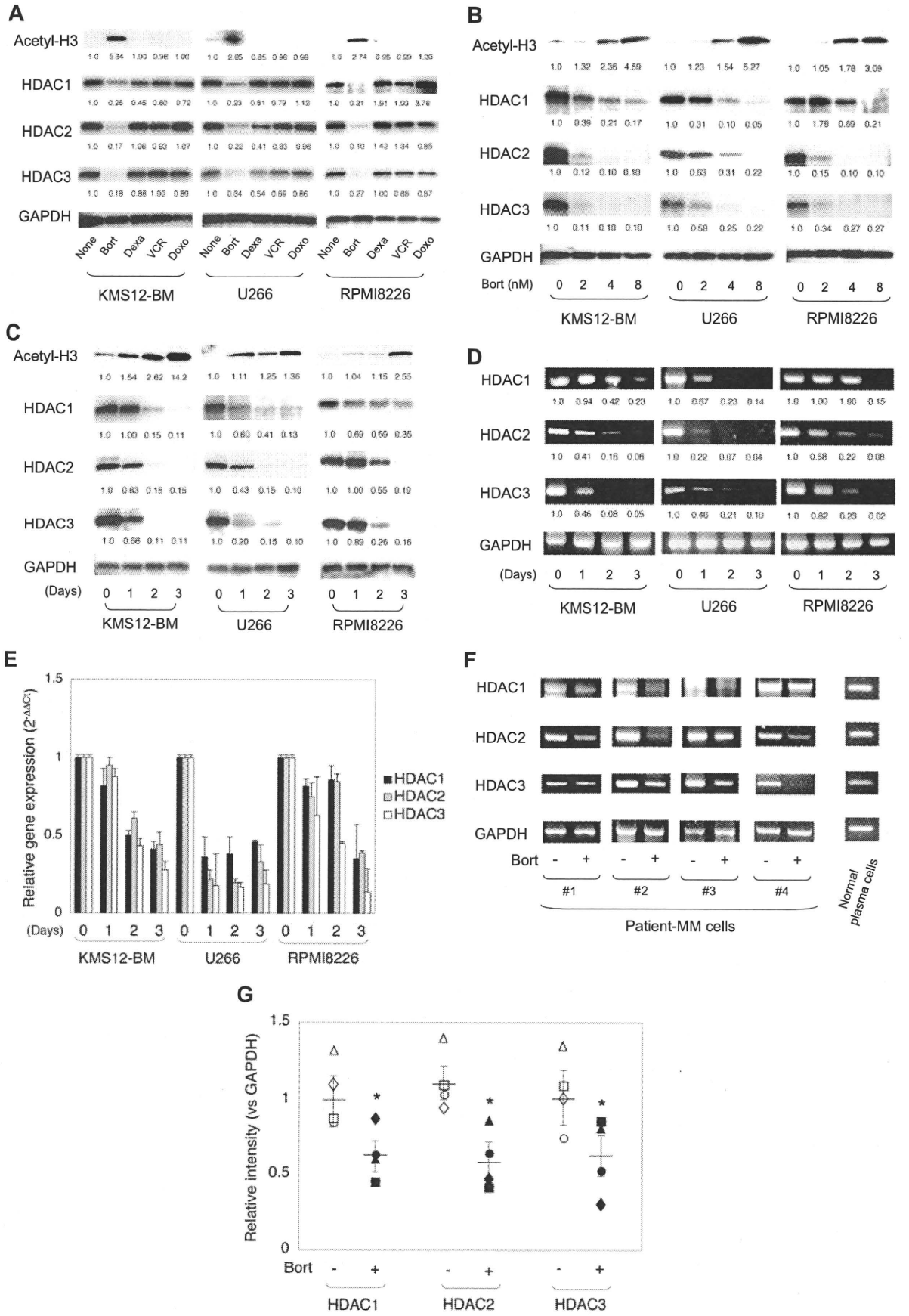

Figure 2.

Semiquantitative or real-time quantitative RT-PCR

Total cellular RNA was isolated from 1 to 10×10^4 cells, reverse-transcribed into cDNA using SuperScript reverse transcriptase and oligo(dT) primers (Invitrogen), and subjected to subsequent semiquantitative reverse transcription–polymerase chain reaction (RT-PCR) or real-time quantitative RT-PCR using Power SYBR Green PCR Master Mix (Applied Biosystems) as described previously.[29] Detailed information of primers, including sequences, corresponding nucleotide positions, and PCR product sizes, is shown in supplemental Table 1 (available on the *Blood* Web site; see the Supplemental Materials link at the top of the online article).

Reporter assays

We amplified the promoter region of the HDAC1 gene (−1170 to +397) by PCR and inserted it into the pGL4.10 firefly luciferase vector (Promega) to generate reporter plasmids.[15] We introduced the reporter plasmids into MM cells along with pGL4.73 Renilla luciferase vector (Promega), which served as a positive control to determine transfection efficiencies, in the presence of either test plasmids encoding Sp1 and MZF-1 or empty vectors by electroporation, as previously described.[15] After 48 hours, firefly and Renilla luciferase activities were discriminately measured using the Dual-Luciferase Reporter Assay System (Promega). The promoterless pGL4-basic vector was used as a negative control. The luciferase activity was normalized by the internal standard and indicated as a relative ratio to the negative control. Expression vectors for MZF-1 and Sp1 were kindly provided by Dr Robert Hromas (University of New Mexico) and Dr Mitsuru Nakamura (National Institute of Advanced Industrial Science and Technology), respectively.

ChIP assays

We used the ChIP-IT Chromatin Immunoprecipitation Kit (Active Motif) to perform chromatin immunoprecipitation (ChIP) assays. In brief, cells were fixed with 1% formaldehyde at 37°C for 5 minutes and sonicated to obtain chromatin suspensions. After centrifugation, supernatants were incubated with antibodies of interest at 4°C overnight. The mixture was then incubated with protein A agarose beads at 4°C for 1 hour, and centrifuged to collect the beads. DNA fragments bound to the beads were purified with vigorous washing and subjected to PCR using primer pairs, as shown in supplemental Table 2.[15]

Construction and production of lentiviral expression vectors

We used a lentiviral short-hairpin RNA/short-interfering RNA (shRNA/siRNA) expression vector pLL3.7 for knockdown experiments.[30] siRNA target sequences were designed to be homologous to wild-type cDNA sequences. Oligonucleotides were chemically synthesized, annealed, terminally phosphorylated, and inserted into pLL3.7 vector. Oligonucleotides containing siRNA target sequences are shown in supplemental Table 3. Scrambled sequences were used as controls.

We also used a lentiviral vector CSII-CMV-MCS-IRES-VENUS (kindly provided by Dr Hiroyuki Miyoshi, RIKEN BioResource Center) for gain-of-function experiments after replacing VENUS with DsRed amplified from pDsRed-expressing vector (Clontech Inc).[27] The resulting construct was designated as the CSII-DsRed vector. We constructed HDAC expression vectors by inserting the coding regions of HDAC1, HDAC2, or HDAC3 cDNA (all provided by Dr Stuart L. Schreiber, Broad Institute of Harvard University and MIT).

These vectors were cotransfected into 293FT cells with packaging plasmids (Invitrogen) to produce infective lentiviruses in culture supernatants. Lentiviruses were then added to cell suspensions in the presence of 8 μg/mL polybrene, and transduced for 24 hours, as previously described.[27]

Xenograft murine model

Mice were inoculated subcutaneously in the right thigh with 3×10^7 MM cells in 1×10^{-4} L of RPMI 1640 medium together with 1×10^{-4} L of Matrigel basement membrane matrix (Becton Dickinson).[31] When tumors were measurable, mice were assigned to 3 treatment groups receiving either the vehicle alone (control), bortezomib alone, or bortezomib plus romidepsin. Bortezomib and romidepsin were given intravenously twice a week via the tail vein at 0.5 mg/kg for 4 weeks and intraperitoneally every other day at 0.25 mg/kg for 2 weeks, respectively.[31,32] The control group received the vehicle (0.9% NaCl) alone on the same schedule. Caliper measurements of the longest perpendicular tumor diameters were performed every alternate day to estimate the tumor volume using the following formula: $4/3\pi \times (\text{width}/2)^2 \times (\text{length}/2)$, which represents the 3-dimensional volume of an ellipse.

Results

Synergistic effects of romidepsin and bortezomib on viability and histone acetylation of MM cells

Romidepsin has proved to be one of the most effective HDAC inhibitors against hematologic malignancies both in vitro and in vivo.[33,34] Initially, we examined the combination of romidepsin and bortezomib to develop an effective treatment strategy for MM, because bortezomib can enhance the effects of other anticancer drugs.[6,30] As anticipated, an isobologram analysis of drug combination revealed that bortezomib and romidepsin showed synergistic cytotoxicity in U266 and RPMI8226 cells (Figure 1A). Next, we investigated the molecular basis of the synergistic effect of the 2 drugs. We speculated that bortezomib enhanced the HDAC inhibitory activities of romidepsin. To test this hypothesis, we determined cellular HDAC activity by monitoring the status of histone acetylation. As shown in Figure 1B, consistent with our hypothesis, bortezomib markedly enhanced romidepsin-induced hyperacetylation of histones H3 and H4. Moreover, we found here that bortezomib not only enhanced the effect of romidepsin but also induced histone hyperacetylation. These results suggest a novel mechanism of bortezomib action: it may induce cytotoxicity in MM cells by HDAC suppression. Although most cellular HDAC

Figure 2. Expression of class I HDACs in MM cells during bortezomib treatment. (A) MM cell lines (KMS12-BM, U266, and RPMI8226) were cultured in the absence or presence of either 4nM bortezomib (Bort), 50nM dexamethasone (Dexa), 1nM vincristine (VCR), or 100nM doxorubicin (Doxo) for 48 hours. Whole-cell lysates were subjected to immunoblotting. (B) MM cell lines were cultured in the absence or presence of bortezomib (Bort) at the indicated doses for 48 hours, or (C) cultured in the presence of 4nM bortezomib for up to 3 days. Whole-cell lysates were prepared at given time points and subjected to immunoblotting. (D) Total cellular RNA was isolated simultaneously in the experiments described in panel C and subjected to semiquantitative RT-PCR analysis for the expression of HDAC1, HDAC2, HDAC3, and GAPDH (internal control). The amplified products were visualized by ethidium bromide staining after 2% agarose gel electrophoresis. The results of suboptimal amplification cycles, 35 cycles, are shown. The signal intensities of each band were quantified, normalized to those of the corresponding GAPDH, and shown as relative values setting day 0 controls to 1.0. (E) Total cellular RNA was isolated simultaneously in the experiments described in panel C and subjected to real-time quantitative RT-PCR. The expression of HDAC1, HDAC2, and HDAC3 was normalized to that of GAPDH and quantified by the $2^{-\Delta\Delta Ct}$ method. The means ± SD (bars) of 3 independent experiments are shown. (F) We cultured primary MM cells in the absence or presence of 2nM bortezomib for 48 hours, and determined the expression of HDAC1, HDAC2, HDAC3, and GAPDH (internal control) transcripts by semiquantitative RT-PCR. PCR amplification was carried out with 1 μL of cDNA solution (corresponding to 500 cells). PCR products were resolved on 2% agarose gels and visualized by staining with ethidium bromide. The results of suboptimal amplification cycles, 40 cycles, are shown. (G) The signal intensities of HDACs were quantified with a densitometer, and their means are shown as a ratio to those of GAPDH in corresponding samples. The values of individual samples isolated in the absence or presence of bortezomib are indicated as follows: patient no. 1, circles; patient no. 2, squares; patient no. 3, triangles; and patient no. 4, diamonds, respectively. Bars indicate the average values of each molecule. *P* values were calculated by 1-way analysis of variance (ANOVA) with the Student-Newman-Keuls multiple comparisons test. $^*P < .05$.

activities rely on class I HDACs, Hideshima et al[35] showed that specific inhibitors of class II HDACs, such as tubacin, synergized with bortezomib via inhibition of HDAC6 activity. We therefore examined the effect of romidepsin on HDAC6 activity by monitoring the status of tubulin acetylation. As shown in supplemental Figure 1, tubulin acetylation was observed only at higher concentrations (> 2nM), indicating that romidepsin inhibits the activities of class I HDACs at lower concentrations and both class I and class II HDACs at higher concentrations. As additive cytotoxicity and histone hyperacetylation were observed with less than 1nM romidepsin, these effects are considered to be achieved mainly via the inhibition of class I HDACs. Thereafter, we focused on this novel

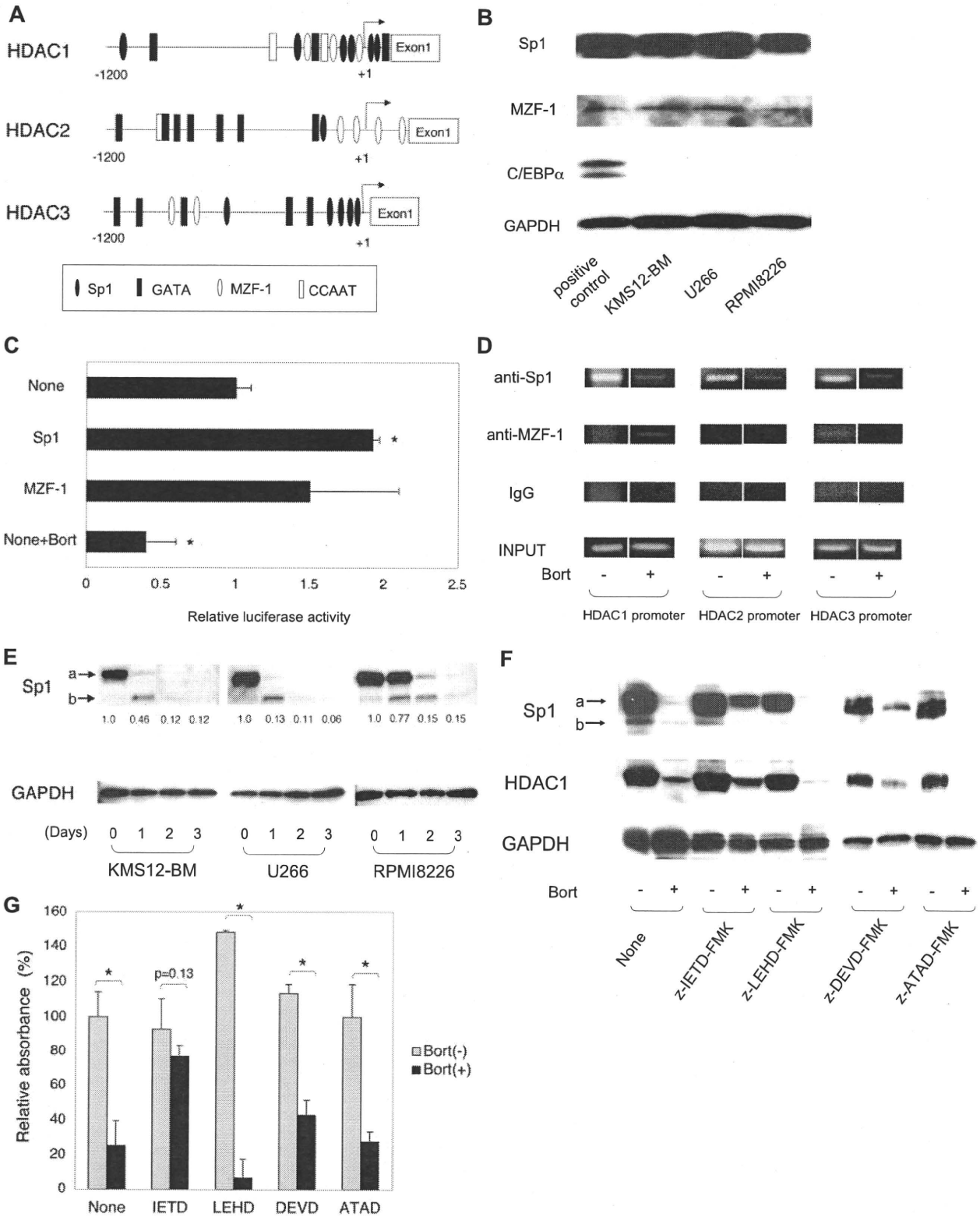

Figure 3.

property of bortezomib and investigated its molecular mechanisms and roles in cytotoxicity against MM.

Down-regulation of HDAC expression in MM cells during bortezomib treatment

First, we investigated the molecular mechanisms of how bortezomib induced histone hyperacetylation in MM cells. We speculated that bortezomib did not inhibit HDAC activity like conventional HDAC inhibitors but down-regulated the expression of class I HDACs, because we and others have shown that bortezomib suppressed the expressions of various molecules, such as CD49d,[30] HLA class I,[36] and DNMT1,[37] in MM cells. To verify this hypothesis, we determined the expression of class I HDACs (HDAC1, HDAC2, and HDAC3) in human MM cell lines (KMS12-BM, U266, and RPMI8226) during bortezomib treatment. We also treated MM cell lines with conventional antimyeloma drugs (vincristine, dexamethasone, and doxorubicin) to be used as control samples. As shown in Figure 2A, along with the induction of histone hyperacetylation, bortezomib readily down-regulated the expression of class I HDACs in all 3 MM cell lines. In contrast, there were no significant changes in histone acetylation and HDAC expression in cells treated with other drugs. The histone hyperacetylation and down-regulation of HDACs were reciprocally induced by bortezomib in a dose- and time-dependent fashion (Figure 2B-C). These results suggest that bortezomib induced histone hyperacetylation via the down-regulation of class I HDACs expression in MM cells.

Next, we determined whether the down-regulation of HDAC expression occurred at transcriptional or posttranscriptional levels. We performed semiquantitative RT-PCR and real-time quantitative RT-PCR in MM cells during bortezomib treatment. As shown in Figure 2D-E, bortezomib down-regulated mRNA levels of HDAC1, HDAC2, and HDAC3 in all 3 MM cell lines in a time-dependent fashion. The suppression pattern was quite similar to that of proteins. In addition, semiquantitative RT-PCR and Western blot analyses revealed that there were no significant changes in the expression of other classes of HDACs, such as HDAC4, HDAC5, HDAC6, and SIRT1 (supplemental Figure 2; data not shown). These results suggest that bortezomib transcriptionally repressed the expression of class I HDACs in MM cells.

In addition, we performed the same experiments using primary myeloma cells: $CD138^+$ cells from BM mononuclear cells of patients with MM. First, primary MM cells (patient no. 3) were cultured in the absence or presence of 2, 4, and 8nM bortezomib for 2 days, followed by semiquantitative RT-PCR analysis. We could detect HDAC1, HDAC2, and HDAC3 transcripts in a semiquantitative manner between 30 and 40 PCR cycles (supplemental Figure 3A), and observed the down-regulation of HDAC expression at more than 2 nM bortezomib (supplemental Figure 3B-C). Based on these preliminary experiments, we cultured primary MM cells in the absence or presence of 2nM bortezomib for 2 days and detected the expression of HDAC genes at 40 PCR cycles. As shown in Figure 2F and G, bortezomib significantly down-regulated the expressions of HDAC1, HDAC2, and HDAC3 in primary myeloma cells, suggesting that bortezomib transcriptionally down-regulated the expressions of class I HDACs in primary MM cells as well as cell lines.

Caspase-8–dependent cleavage of Sp1 protein underlies transcriptional repression of HDAC genes by bortezomib

Next, we investigated the mechanisms of transcriptional repression of HDAC genes during bortezomib treatment in MM cells. As illustrated in Figure 3A, there are a number of putative transcription factor binding sites in the promoter regions of class I HDAC genes. We have previously shown that Sp1 and GATA1 are potent transcriptional activators, and MZF-1, GATA2, and C/EBPα are repressors for HDAC1 transcription in myeloid cells.[15] We initially screened for the expression of these factors in MM cells, and identified the expression of Sp1 and MZF-1 but not GATA1, GATA2 and C/EBPα (Figure 3B; data not shown). Therefore, we focused on Sp1 and MZF-1 as transcriptional regulators of HDACs in MM cells. Because their binding sites are commonly observed in the promoter regions of 3 HDAC genes, we speculated that HDAC transcription was regulated in a similar manner in MM cells. First, we examined the transcriptional activity of the HDAC1 promoter in KMS12-BM cells by reporter assays using the segment between −1179 and +397 of the HDAC1 gene, which confers full promoter activity.[15] As shown in Figure 3C, overexpression of Sp1 significantly increased HDAC1 promoter activity, whereas MZF-1 failed to do so, indicating that Sp1 acts as a transcriptional activator in KMS12-BM cells. In addition, bortezomib was shown to modify the transcriptional activity in this system (Figure 3C). We also examined the transcriptional activity of the HDAC3 promoter in KMS12-BM cells. Reporter assays revealed that promoter activity was enhanced by Sp1 but not MZF-1, suggesting that Sp1 transactivates HDAC3 as well as HDAC1 (data not shown). Furthermore, bortezomib also reduced HDAC3 promoter activity (data not shown). Taken together, Sp1 is a major transcriptional activator of class I HDAC genes in MM cells.

Figure 3. Regulation of HDAC1 promoter by Sp1 transcription factor. (A) Schematic representations of HDAC1, HDAC2, and HDAC3 promoter constructs are shown. Relative locations of the putative binding sites of hematopoietic transcription factors are approximated by the symbols shown in the box. (B) Whole-cell lysates were prepared from MM cell lines and subjected to immunoblotting. HEK293 cells were transduced with expression vectors encoding Sp1, MZF-1, and C/EBPα, and used as positive controls. (C) We transfected 10 μg of pGL4.10 plasmid containing HDAC1 promoter sequences between −1170 and +397 into KMS12-BM cells along with 10 μg of expression vectors encoding Sp1 and MZF-1, and measured luciferase activities after 48 hours. HDAC1 promoter activity was calculated as firefly luciferase activities of cells transfected with an empty expression vector set at 1.0 after normalization of transfection efficiencies using Renilla luciferase activities. Data shown are the means ± SD of 3 independent experiments. *P* values were calculated by 1-way ANOVA with Student-Newman-Keuls multiple comparisons test. $^*P < .05$. (D) KMS12-BM cells were cultured in the absence or presence of bortezomib for 2 days and subjected to ChIP assays. Chromatin suspensions were immunoprecipitated with the indicated antibodies and corresponding control antibodies. The resulting precipitants were subjected to PCR to amplify the promoter regions of the HDAC genes. The amplified products were visualized by ethidium bromide staining after 2% agarose gel electrophoresis. Representative data of 50 cycles are shown. Input indicates that PCR was performed with genomic DNA. (E) Whole-cell lysates were isolated simultaneously in the experiments described in Figure 2C, and subjected to immunoblotting. Arrows "a" and "b" indicate the intact and cleaved bands of Sp1, respectively. The signal intensities of each band were quantified, normalized to those of the corresponding GAPDH, and shown as relative values setting day 0 controls to 1.0. (F) KMS12-BM cells were cultured with the indicated combinations of 8nM bortezomib (Bort), 100μM z-IETD-FMK (caspase-8 inhibitor), 100μM z-LEHD-FMK (caspase-9 inhibitor), 50μM z-DEVD-FMK (caspase-3 inhibitor), and 20μM z-ATAD-FMK (caspase-12 inhibitor) for 48 hours. Whole-cell lysates were subjected to immunoblotting. (G) Cell viability was determined with a Cell Counting Kit (WAKO) after culturing MM cells in the absence or presence of 8nM bortezomib (Bort) with or without either 100μM z-IETD-FMK (IETD) or 100μM z-LEHD-FMK (LEHD) for 48 hours. Absorbance at 450 nm was measured with a microplate reader, and expressed as a percentage of the value of the corresponding untreated cells. The means ± SD (bars) of 3 independent experiments are shown. *P* values were calculated by 1-way ANOVA with the Student-Newman-Keuls multiple comparisons test. $^*P < .05$.

Next, we performed ChIP assays to investigate the binding of these transcriptional regulators to HDAC promoters in vivo and their changes during bortezomib treatment. We detected the binding of Sp1 to HDAC1, HDAC2, and HDAC3 promoter regions in untreated KMS12-BM cells, whereas Sp1 dissociated from all 3 promoters upon bortezomib treatment (Figure 3D). Although MM cells expressed MZF-1, we could not detect its binding to promoters. These results suggest that Sp1 confers the baseline expression of HDAC genes.

To clarify the mechanisms of changes in promoter binding, we detected the expression of Sp1 protein in MM cell lines during bortezomib treatment. As shown in Figure 3E, bortezomib markedly down-regulated the expression of Sp1 in all 3 MM cell lines in a time-dependent fashion. In addition, we found that an extra signal (indicated by arrow "b" in Figure 3E) appeared below the major signal of Sp1 protein (indicated by arrow "a" in Figure 3E) in bortezomib-treated cells. Previous studies showed that Sp1 protein was cleaved and degraded by caspases such as caspase-8, caspase-9, and caspase-3,[38] and bortezomib activated caspase-8, caspase-9, caspase-3, and caspase-12.[39-41] On this basis, we hypothesized that the extra signal was caspase-cleaved Sp1 protein. To confirm this hypothesis, we cultured KMS12-BM cells with peptide inhibitors of caspase-8 (z-IETD-FMK), caspase-9 (z-LETD-FMK), caspase-3 (z-DEVD-FMK), and caspase-12 (z-ATAD-FMK) in the absence or presence of bortezomib, and examined the expression of Sp1 protein. As shown in Figure 3F, IETD but not other inhibitors perturbed the bortezomib-induced down-regulation of Sp1. In KMS12-BM cells, caspase-8 activation occurred 12 hours after bortezomib exposure, which was accompanied by reciprocal down-regulation of Sp1 expression (supplemental Figure 4). These results suggest that caspase-8 is responsible for the cleavage and degradation of Sp1 protein in bortezomib-treated cells. In parallel with the restored Sp1 expression, the caspase-8 inhibitor blocked the down-regulation of HDAC expression in KMS12-BM cells. In addition, IETD but not other caspase inhibitors could abrogate bortezomib-induced cytotoxicity in KMS12-BM cells in a dose-dependent fashion (Figure 3G; supplemental Figure 5). These results suggest that bortezomib degraded Sp1 protein via the caspase-8–dependent pathways, leading in turn to the transcriptional repression of HDAC genes in MM cells. In line with our observation, Hideshima et al[39] reported that caspase-8 is a primary initiating caspase in bortezomib-mediated cell death. Taken together, our results suggest that the caspase-8/Sp1/HDAC axis is a critical pathway for bortezomib-mediated cytotoxicity in MM cells.

Increased cytotoxicity of bortezomib by shRNA/siRNA-mediated knockdown of HDAC1 expression

To confirm the roles of HDACs in bortezomib-induced cytotoxicity, we performed loss-of-function analysis using the shRNA/siRNA lentivirus system.[30] We could achieve significant loss-of-function of HDACs by solely targeting HDAC1, because HDAC1 represents more than half of all cellular HDAC activities, and other HDACs cannot compensate for the loss of HDAC1.[11] We constructed lentiviral shRNA/siRNA expression vectors (supplemental Figure 6A) and transfected them into 3 MM cell lines for further analyses. As shown in Figure 4A, specific reduction of HDAC1 expression was confirmed by Western blotting in GFP$^+$ cells collected by a cell sorter. Upon transduction with shRNA, we determined apoptosis induction in the absence or presence of bortezomib. As shown in Figure 4B, HDAC1 knockdown slightly increased apoptosis in untreated MM cells, but the effect was not statistically significant compared with inactive sh-controls. With bortezomib treatment, however, HDAC1 knockdown significantly increased apoptosis in 3 MM cell lines; this effect was observed at various doses of bortezomib (supplemental Figure 7A). Cell proliferation assays and BrdU/7-AAD double staining revealed that HDAC1 knockdown only marginally affected growth rate and cell-cycle patterns (supplemental Figure 7B-C). These results

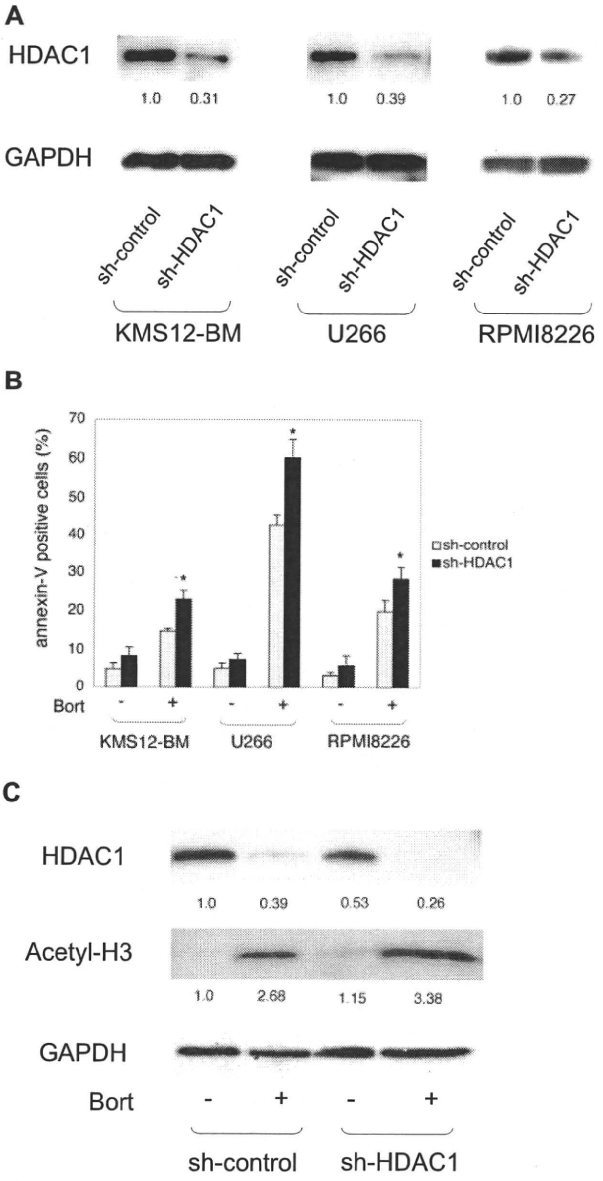

Figure 4. Effects of shRNA-mediated knockdown of HDAC1 on bortezomib-induced apoptosis in MM cells. (A) MM cell lines were transfected with either pLL3.7-sh-HDAC1 (sh-HDAC1) or sh-control vector. Whole-cell lysates were prepared from GFP$^+$ cells collected using a FACSAria flow cytometer and subjected to immunoblotting. The signal intensities of each band were quantified, normalized to those of the corresponding GAPDH, and shown as relative values setting the sh-control to 1.0. (B) MM cell lines transfected with shRNA vectors were cultured in the absence or presence of 2nM bortezomib. After 48 hours, MM cells were harvested, stained with annexin-V/APC, and subjected to flow cytometric analysis. The y-axis shows the proportion of annexin-V positivity in the GFP$^+$ fraction. The means ± SD (bars) of 3 independent experiments are shown. *P* values were calculated by 1-way ANOVA with the Student-Newman-Keuls multiple comparisons test. $^*P < .05$ against the sh-control. (C) shRNA-transduced RPMI8226 cells were cultured in the absence or presence of 2nM bortezomib. After 48 hours, whole-cell lysates were prepared from GFP$^+$ cells collected by the FACSAria flow cytometer, and subjected to immunoblotting. The signal intensities of each band were quantified, normalized to those of the corresponding GAPDH, and shown as relative values setting the untreated sh-control to 1.0.